Department of Chemistry and Pharmacy
Johannes-Gutenberg University
Mainz

Glutamate-Induced Potentiation of Calcium Influx in Primary Hippocampal Culture Neurons

- Doctoral Thesis –

Vojislav Pejovic
born in Podgorica, Yugoslavia

Mainz, 2001

TABLE OF CONTENTS

LIST OF ABBREVIATIONS

AChE	Acetylcholine esterase
ACPD	(1S, 3R)-1-Aminocyclopentane-1,3-dicarboxylic acid
AD	Alzheimer's disease
AMPA	(S)-α-Amino-3-hydroxy-5-methyl-4-isoxazolepropionic acid
AMPAR	(S)-α-Amino-3-hydroxy-5-methyl-4-isoxazolepropionic acid receptor
AP-4	L(+)-2-Amino-4-phosphonobutyric acid
AP-5	D(-)-2-Amino-5-phosphonopentanoic acid
CA1	*Cornu Ammoni 1*
CA3	*Cornu Ammoni 3*
CaMKII	Calcium-calmodulin kinase II
cAMP	Cyclic adenosine monophosphate
CCD	Charge-coupled device
CNQX	6-Cyano-7-nitroquinoxaline-2,3-dione
DAG	Diacyl glycerol
DMSO	Dimethyl sulfoxide
EGTA	[Ethylene-bis(oxyethylenenitrilo)]tetraacetic acid
EPSPs	excitatory postsynaptic potentials
FCS	Fetal calf serum
Fura-2 AM	5-Oxazolecarboxylic acid, 2-(6-(bis(2-((acetyloxy)methoxy)-2-oxoethyl)amino)-5-(2-(2-(bis(2-((acetyloxy)methoxy)-2-oxoethyl)amino)-5-methylphenoxy)ethoxy)-2-benzofuranyl)-,(acetyloxy)methyl ester
GABA	γ-Amino-n-butyric acid
GABAR	γ-Amino-n-butyric acid receptor
Gal	Galanthamine ((4a,5,9,10,11,12-Hexahydro-3-methoxy-11-methyl-6H-benzofuro[3a,3,2-ef][2]benzazepin-6-ol)
HEPES	N-(2-Hydrohyethyl)piperazine-N'-(2-ethanesulfonic acid)
IPSPs	Inhibitory postsynaptic potentials
KW	Kruskal-Wallis (statistics)
LTD	Long-term depression
LTP	Long-term potentiation
LY341495	2S-2-Amino-2-(1S,2S-2-carboxycyclopropyl-1-yl)-3-(xanth-9-yl)propanoic

	acid
MCPG	(S)-α-Methyl-4-carboxyphenylglycine
mGluR	Metabotropic glutamate receptor
MK-801	((5R,10S)-(+)-5-Methyl-10,11-dihydro-5H-dibenzo[a,d]cyclohepten-5,10-imine
MOPS	3-(M-Morpholino)butanesulfonic acid
nAChR	Nicotinic acetylcholine receptor
Nic	Nicotine ((-)-1-Methyl-2-(3-pyridyl)pyrrolidine)
Nif	Nifedipine (1,4-Dihydro-2,6-dimethyl-4-(2-nitrophenyl)-3,5-pyridinedicarboxylic acid dimethyl ester
NMDA	N-Methyl-D-aspartic acid
NMDAR	N-Methyl-D-aspartic acid receptor
PAF	Platelet-activated factor
PBS	Phosphate buffer saline
PKA	Protein kinase A
PKC	Protein kinase C
PSD	Postsynaptic density
Riv	Rivastigmine
ROM	Read-only memory
TEA	Tetraethyl ammonium- (chloride)
UV	Ultraviolet (light)
VGCC	Voltage-gated calcium channel

1. INTRODUCTION

1.1 Memory, Hebb's rule, hippocampus

The word „memory**"** is used to name the ability of a system to store and retrieve once acquired information. (The very process of information acquisition is usually described as „learning", and is functionally inseparable from information storage.) Extensive research in the various fields of human activity – *e.g.* psychology, biology or computer science - gave rise to diversification of the term „memory" itself, making it necessary to differentiate, for example, between the **procedural**, **working**, or the **ROM** one. Psychologists were able to make several useful distinctions related to the subject: **Declarative** memory is a „memory of facts", i.e. learning poems by heart or studying maths. **Procedural** memory is memory for skills or behaviour (tying the shoes, for example). **Short-term** memory is an ability that requires continual rehearsal, has short duration and rather limited capacity. Quite opposite qualities are the characteristics of the **long-term** memory; whereas the process that enables the former to become the latter is named **consolidation**. **Working** memory would be a broader-scope version of the short-term memory, and allows for the possibility that several types of information are held simultaneously (*e.g.* playing a musical instrument)[1].

In 1949, the Canadian psychologist Donald Hebb published a book „Organization of Behavior", which contains the most valuable model of memory formation in the brain so far. According to Hebb, a memory trace - or an **engram** - is the result of a simultaneous activation of a group (or „assembly") of neurons, exposed to an external stimulus. These neurons are interconnected by „plastic" synapses, which can change their "strength" if the stimulus persists long enough. This "strengthening" leads to the consolidation of cell-cell interactions, and repetition of the former (even incomplete) stimulus is able to activate the whole assembly again. An engram could be (1) widely distributed among the neurons' interconnections, and (2) could involve the same neurons that take part in sensation and perception. Hebb's hypothesis (also known as: „cells that fire together, wire together") is illustrated in **Figure 1**. However, the hypothesis remained without an experimental proof up to the early seventies (*vide infra*), when research on long-term potentiation (LTP) in the hippocampus provided an appropriate, realistic, experiment-based context.

The role of the hippocampus in memory formation has been extensively demonstrated, and ranges from declarative memory consolidation to sensory discrimination and spatial tasks. The hippocampal structure is a part of the diencephalon, and receives inputs from the associa-

[1] Different types of memory mentioned in this paragraph are merely to illustrate how widely this term is used.

tive neocortex *via* the entorhinal cortex, through a bundle of axons described as the **perforant pathway**. These axons synapse with the granule cells of the dentate gyrus, whereas the dentate gyrus axons (the **mossy fibers**) protrude to the hippocampus proper and make synapses with the large pyramidal cells of the **CA3** region (which also receive direct input from the perforant pathway). Branches of CA3 pyramidal cell axons - named **Schaffer collaterals** – project onto smaller pyramidal cells of the **CA1** region, whose axons return to the neocortex. This neuro-circuitry can be observed in every cross-section of the hippocampus.

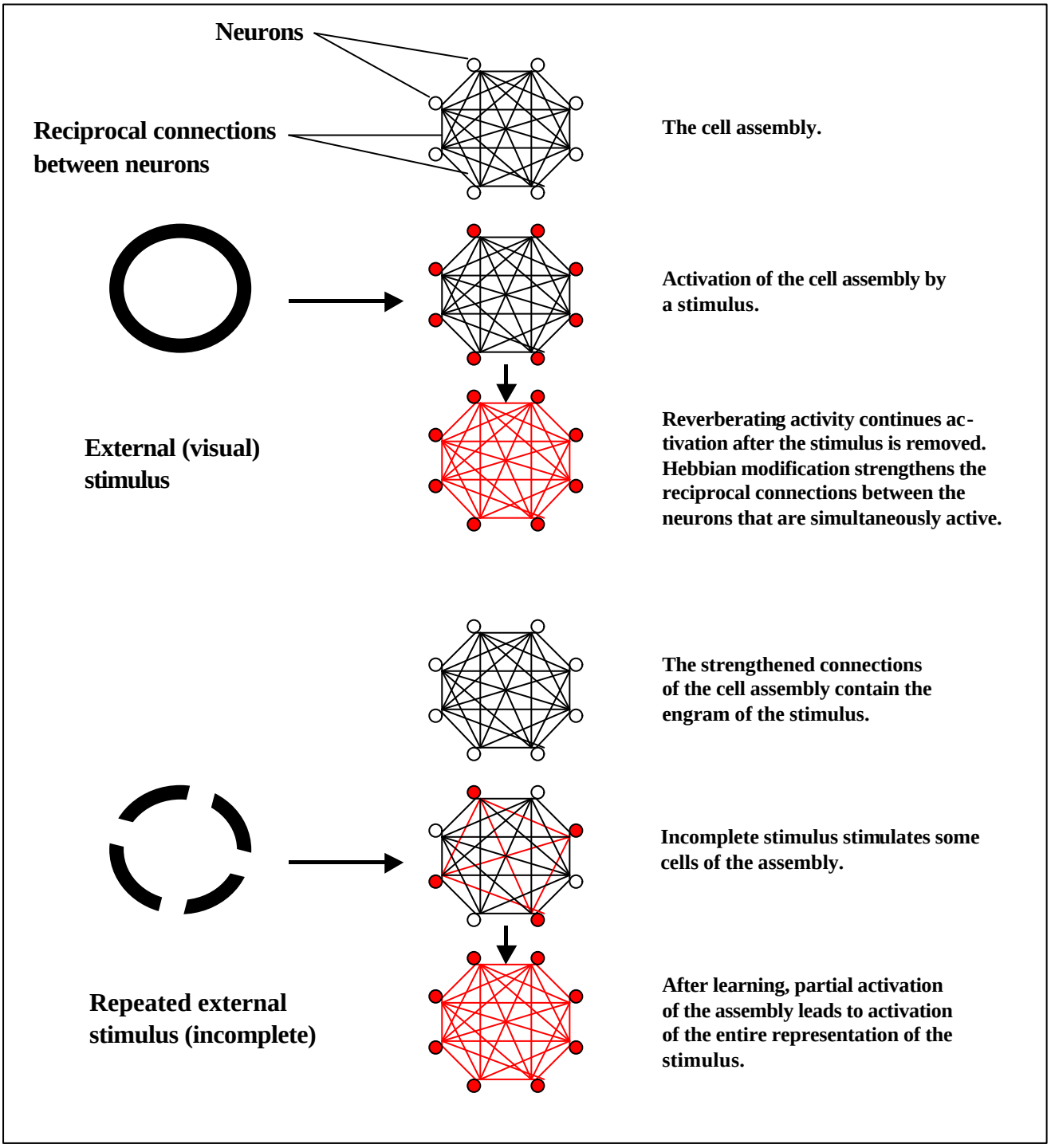

Figure 1. Illustration of the Hebb's rule (from Bear, Connors and Paradiso, 1994).

Each of these cells is glutamatergic, with the NMDA subtype of glutamate ionotropic receptors being particularly abundant in zones containing the dendrites of dentate gyrus' granule cells and CA1 pyramidal neurons (Ikonomovic *et al*., 1999). Aside those major pathways, the hippocampus also contains numerous GABAergic interneurons, receiving axon collaterals from the glutamatergic neurons and thus mediating inhibition via $GABA_A$ (fast IPSPs, ionotropic) and $GABA_B$ (slow IPSPs, metabotropic) receptors. A schematic drawing of the hippocampus location in the brain, a cross section of it and its generalized circuitry are depicted in **Figure 2**.

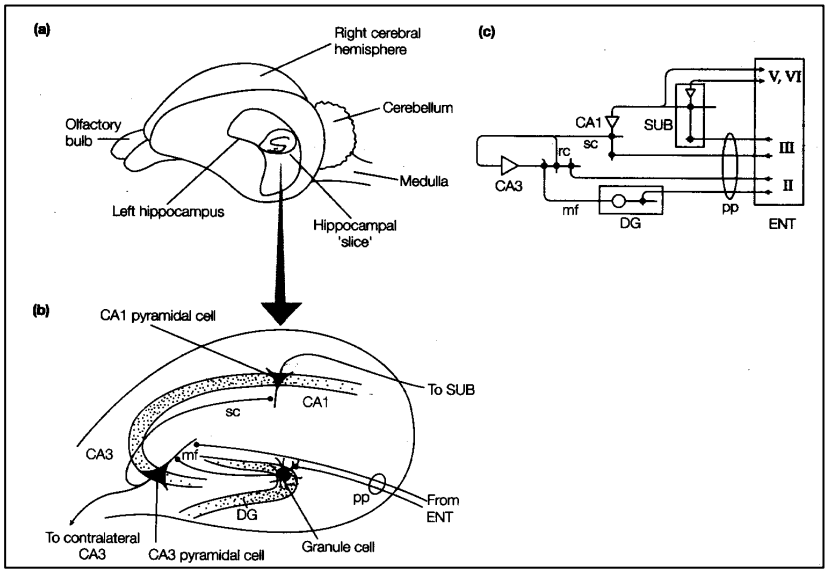

Figure 2. Hippocampus: its location in rat brain (a), cross section (b) and schematic circuitry (c). DG, dentate gyrus, ENT, enthorinal cortex; mf, mossy fiber; pp, perforant pathway; rc, recurrent collateral; sc, Schafer collateral; SUB, subiculum (from Revest and Longstaff, 1998).

1.2 LTP – a definition

Long-term potentiation (LTP) is a term coined in the seventies, as a result of initial discoveries made by Terje Lømo of Norway in the mid sixties (Lømo, 1966), and his subsequent collaboration with Tim Bliss and A.R. Gardner-Medwin of England (Bliss and Lømo (a), 1970, Bliss and Lømo (b), 1973, Bliss and Gardner-Medwin, 1973, Gardner-Medwin and Lømo, 1973). The fact that the granule cells of the rabbit hippocampus showed increased responsiveness to an electric stimulus as a result of stimulation of their afferent pathway came as a first experimental support of the hypothesis postulated by Hebb in 1949. This "potentiated" efficacy of synaptic transmission in response to brief trains of high-frequency stimulation of excitatory pathways can be elicited in all pathways of the hippocampus,

either in slices or - by implanted electrodes - in anesthetized or conscious behaving animals. Nowadays, the best understood form of LTP is the one of CA3-CA1 synapses, with its properties fitting very well into Hebb's hypothesis. LTP in other brain regions is also well documented, but it is not always of Hebbian type.

Figure 3. depicts the experimental set-up, generally used to measure increased synaptic transmission in hippocampal slices.

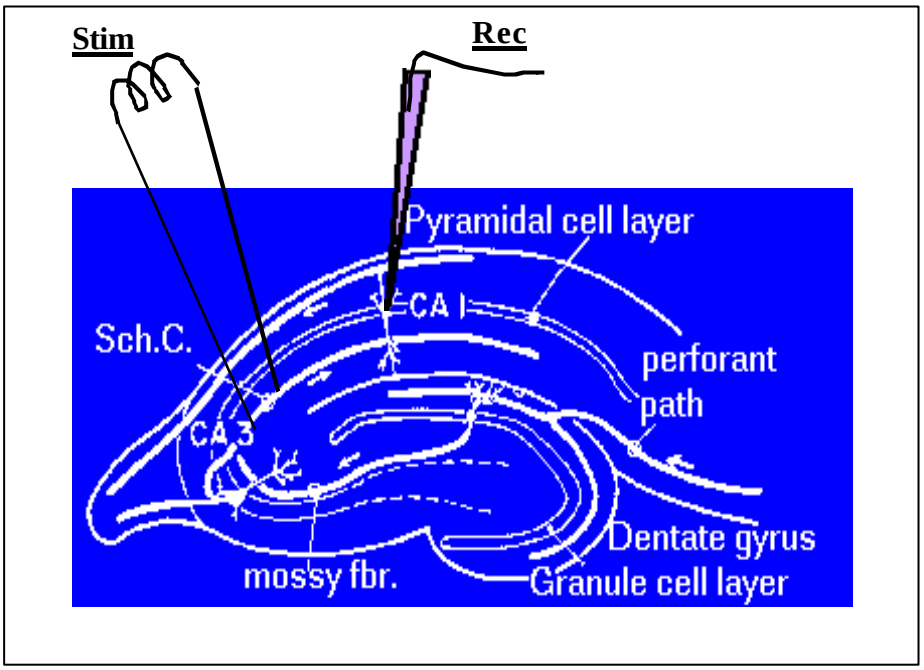

Figure 3. Schematic drawing of an LTP stimulation – recording scheme in hippocampal slice. Stim – stimulation electrode; Rec – recording electrode. Sch.C. – Schaffer collateral. Mossy fbr. – mossy fibres.)

Induction of LTP is usually performed by applying tetanic stimulus (*e.g.* 100 stimuli of 100 Hz) to an afferent pathway. The response is recorded either from an individual neuron or from a population of cells. The feature commonly monitored is a rise in the slope of the field EPSPs, which can last for hours in anesthetized animals or *in vitro*, but days in freely moving animals (**Figure 4**).

The firing pattern that is produced in the hippocampus of the rat, when exploring a novel environment, happens to be very effective in inducing LTP. This pattern (named **theta rhythm**) is normally generated in the septal nucleus, a structure that has an extensive projection to the hippocampus. The theta rhythm consists of bursts of four action potentials at 100 Hz frequency, separated by intervals of approx. 200 ms.

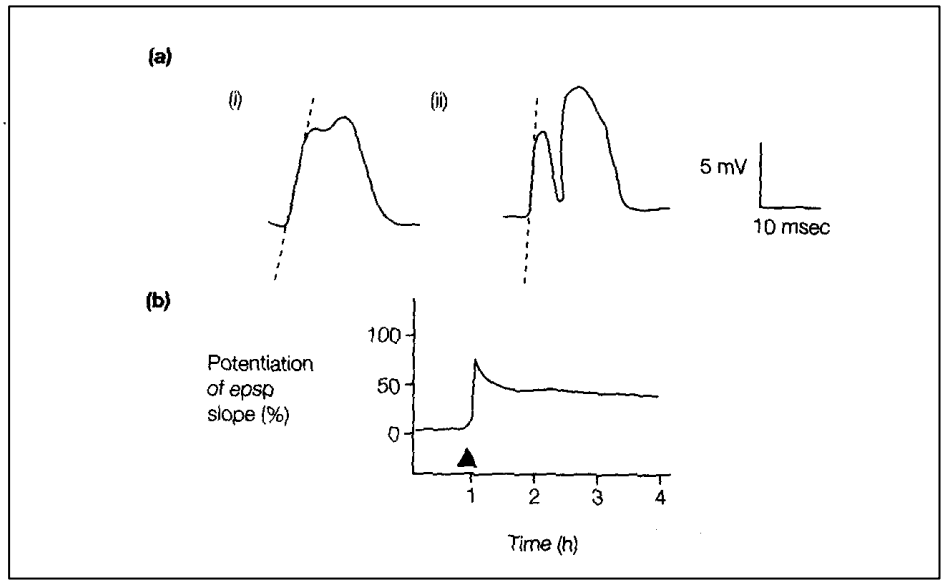

Figure 4. Rcecordings of LTP from rat hippocampus *in vivo*. (a) Extracellular recordings from the CA3 pyramidal cell layer (i) before and (ii) after tetanic astimulation (dashed line: slope of e.p.s.p.); (b) potentiation of the rising phase of the field EPSPs after tetanus (full triangle) (from Revest and Longstaff, 1998).

1.3 LTP - the cascade of events

As mentioned above, all major populations of hippocampal cells are glutamatergic by nature. Receptors for L-glutamate fall into two major classes: ligand-gated ion channel (**NMDA**-, **AMPA**- and **kainate/quisqualate**- type) and metabotropic, G-protein coupled (**mGluRs**) receptors. Both classes have been shown to participate in LTP-related processes, but their actual role depends on the very LTP type involved. LTP can be both **associative** (Hebbian) and **non-associative**, and these two forms seem to use rather different mechanisms (Kandel, Schwartz and Jessel, 2000) . Glutamatergic synapses in the hippocampus exhibit one or the other type. LTP may be NMDAR-dependent or independent, with NMDAR-dependent LTP being usually (but not invariably) associative, and NMDAR-independent being non-associative. Associative LTP is observed at most synapses in the hippocampus, but not those between granule cell mossy fibers and CA3 pyramidal cells (Revest and Longstaff, 1998).

- Induction of LTP

The involvement of NMDARs in associative LTP has been unambiguously demonstrated by the fact that induction of LTP is blocked by NMDAR antagonists, such as AP-5 or MK-801 (Collingridge *et al.*, 1983a, b). Their major functional property is the ability to act as "coincidence detectors" (Hebb, 1949). Namely, in order to open its ion channel and allow the

flux of calcium ions into the dendrites, NMDARs require two conditions to be fulfilled: 1) removing the voltage-dependent Mg^{2+} block and 2) binding of the neurotransmitter. (The requirement (1) is met *in vivo* by strong depolarisation of the postsynaptic cell (Collingridge *et al*., 1988 a,b) and can be additionally met *in vitro* by reducing/omitting magnesium ions from the perfusate (Herron *et al*., 1985). This double-switch action allows the associative LTP to take place.

LTP induction *in vitro* is enhanced at low Mg^{2+} concentrations in the bathing medium, and blocked by low external Ca^{2+} concentration. Also, LTP induction can be prevented by properly timed hyperpolarizing pulses, and it is facilitated by blocking postsynaptic inhibition using $GABA_AR$ antagonists. (GABA, being an inhibitory neurotransmitter, hyperpolarizes the postsynaptic cell, thereby decreasing the probability of LTP induction, see **Figure 5**) (Revest and Longstaff, 1998). Once induced, subsequent **expression of LTP** (persistent increase of cell responsiveness, mediated usually by AMPARs) cannot be blocked any more by NMDAR antagonists, therefore strongly indicating that maintenance of LTP depends on receptors other than NMDARs (*ibid.*).

The events that lead to LTP induction are illustrated in **Figure 5**, both under conditions of low- and high-frequency stimulation of Schaffer collaterals (CA3 axons projecting onto CA1 cell bodies). A single stimulus evokes an EPSP in the postsynaptic CA1 cell which can been blocked by AMPA/kainate receptor antagonists such as 6-cyano-7-nitroquinoxaline-2,3-dione (CNQX). It is rapidly "extinguished" by a biphasic IPSP, caused by excitation of GABAergic interneurons resulting in the activation of $GABA_A$ and, subsequently, $GABA_B$ receptors. Under such circumstances, the probability of activation of NMDARs is low, due to incomplete lift of their voltage-dependent Mg^{2+} blockade by the brief depolarization (*ibid.*).

Exposing Schaffer collaterals to a high-frequency tetanic stimulus creates a rather different scenario. It results in a sustained depolarization, required for activation of (comparably slower) NMDARs as well: glutamate binds to the receptor, with the decrease in the membrane potential being large enough to push Mg^{2+} away from the open channel, thereby allowing Ca^{2+} influx. These conditions are exactly of the kind demanded by Hebb's rule, *i.e.* simultaneous coactivation of a presynaptic (glutamate release) and a postsynaptic (large depolarization) cell (ibid.).

There exist several possibilities that could lead to large depolarisation generated by high-frequency stimulation: (a) tetanus, by inducing sustained glutamate release, causing summation of AMPAR-mediated EPSPs; (b) GABAergic inhibition, which might become less powerful

due to raised concentrations of intracellular Cl^- and extracellular K^+ (prolonged activation of $GABA_A$ and $GABA_B$ (K^+-channel activity affecting) receptors, causing the equilibrium potentials for these ions to shift in the direction of depolarization); (c) $GABA_B$ autoreceptors, located on inhibitory nerve terminals, which may lead to reduced GABA release, thus reducing inhibition. (The third mechanism remains inactive at low-frequency stimulation, since it takes over 10 ms to develop; *ibid.*)

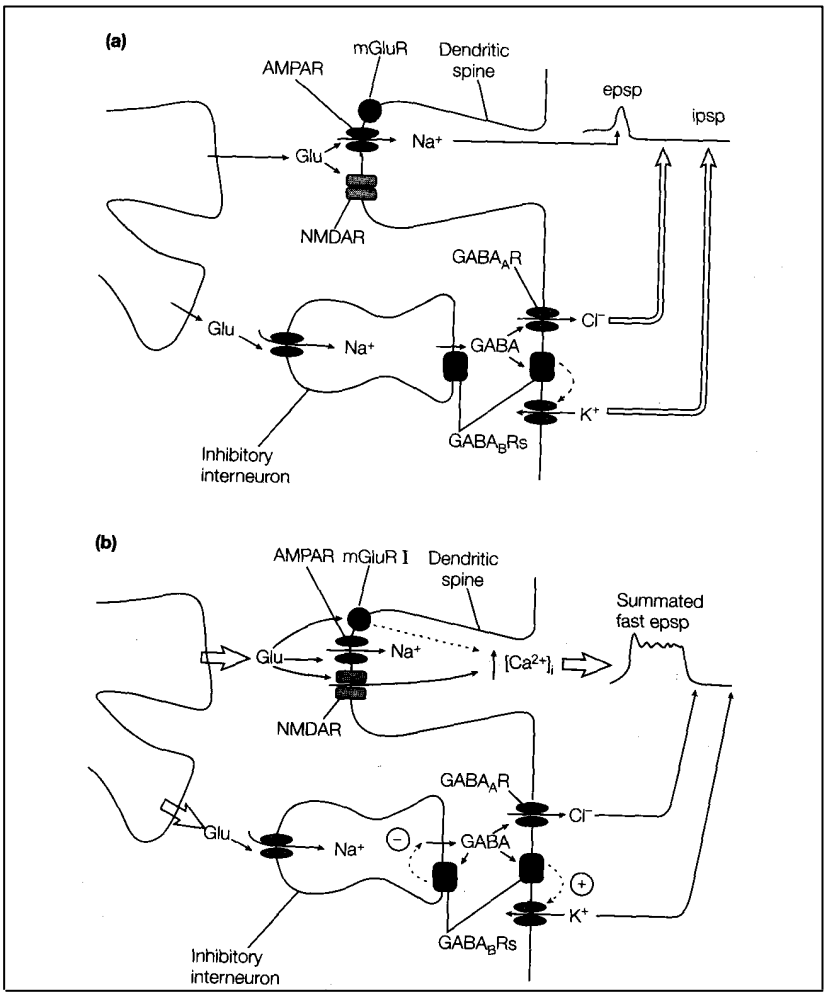

Figure 5. Neurotransmitter systems in LTP during (a) low-frequency and (b) high-frequency (tetanic) stimulation, respectively (from Revest and Longstaff, 1998).

- *Role of calcium ions*

Involvement of calcium ions in LTP is supported by a large body of convincing evidence. Induction of LTP can be blocked by intracellular injection of EGTA, a Ca^{2+} chelator (Lynch *et al.*, 1983). Ca^{2+} imaging, coupled with whole-cell patch clamping shows that tetanic stimuli which activate NMDAR currents are able to produce increases in intracellular calcium

concentration in dendritic spines. However, influx of extracellular calcium ions apparently is not the only way by which the cytosolic Ca^{2+} levels may rise during LTP. Release of calcium ions from intracellular stores has also been demonstrated to contribute, since thapsigargin, a drug which depletes Ca^{2+} stores, can also block LTP (Reyes and Stanton, 1996). This effect is probably related to the activation of G-protein–coupled, metabotropic GluRs I and V, which also play a prominent role in LTP (*vide infra*).

- *Role of protein kinases*

If the mechanism of LTP maintenance is postsynaptic by nature (and in most of the cases it is, but see below), it would mean that either the number or sensitivity of receptors involved in LTP expression is increased. Both of these parameters could be influenced by phosphorylation of the receptors and/or cytoskeletal proteins, triggered by activating second messenger systems. Both AMPA and NMDA receptors have consensus sequences for phosphorylation sites for a variety of protein kinases (Swope *et al.*, 1999), and there is a significant body of experimental evidence supporting the hypothesis of activated kinases during LTP (Liu *et al.*, 1999; Powell *et al.*, 1994; Klann *et al.*, 1991).

Already in 1987, it was discovered that induction and maintenance of LTP in the intact hippocampus could be blocked by non-specific inhibitors of protein kinases, which led to the suggestion that **protein kinase C** (**PKC**) was a major target (Lovinger *et al.*, 1987). The role of PKC has been more directly demonstrated by using inhibitor peptides that block the enzyme's sites at the receptors. The PKC inhibitor peptide, PKC_{19-31}, blocks the induction of LTP, as do antibodies generated against several PKC isoforms (Wang and Feng, 1992). If injected into postsynaptic neurons, active PKC is able to produce synaptic potentiation (Hu *et al.*, 1987).

PKC, if activated by **diacylglycerol** (**DAG**), may remain active long after the second messenger concentrations have fallen to baseline. This autonomous activation is the appropriate feature for a molecule expected to convert a transient signal into a stable change. Several mechanisms have been identified, where persistent activation of PKC takes place (Sessoms *et al.*, 1992-93). The fact that peptide inhibitors (including PKC_{19-31}) have been shown to reverse LTP even several hours after induction represents solid evidence for sustained PKC activity. This conclusion is further strengthened by observations that PKC substrates remain phosphorylated long after LTP induction (Klann *et al.*, 1993).

Calcium/calmodulin-dependent protein kinase II (**CaMKII**) is another obvious candidate for an involvement in LTP since it is activated by calcium ions and because, like PKC, it can remain persistently active after the Ca^{2+} signal has decayed. Inhibitors of CaMKII and inhibitors of calmodulin also prevent the induction of LTP (Malinow *et al.*, 1988). CaMKII is second messenger-independent already 5 min after tetanic stimulation, and both *in vitro* and *in vivo* studies have shown an increase in the mRNA for the α-, but not for the β-isoform of the enzyme. The former appears to follow, in a time scale-consistent manner, the distribution through the dendrites of the postsynaptic cell. The α-isoform of CaMKII is a major component of the **postsynaptic density** (**PSD**), which makes the enzyme ideally placed for both activation by Ca^{2+} influx and phosphorylation of targets in the postsynaptic membrane (Ouyang *et al.*, 1999). Hippocampal slices from transgenic mice lacking CaMKII show severe deficits in LTP (Stevens *et al.*, 1994).

- *Role of metabotropic GluRs*

Use of weak mGluR agonists enables subthreshold tetani to induce LTP, and the type I/V mGluR specific antagonist **(+) a -methyl-4-carboxyphenylglycine** (**MCPG**) prevents induction of LTP at Schaffer collateral-CA1 synapses in hippocampal slices (Bashir *et al.*, 1993). These results support the hypothesis of mGluRs being involved in LTP. Additionally, the involvement in LTP of PKC and the need of calcium release from internal stores suggest that metabotropic GluRs required for LTP induction might belong to group I. However, studies carried out with knockout mice lacking mGluR1 were inconsistent, having shown both defective and normal LTP.

A classical approach has been much more informative: studies performed by Bortolotto *et al.* in 1994 demonstrated that **sub-maximal** LTP (induced by a single tetanus, which activates both NMDARs and mGluRs) prevents MCPG from blocking the induction of further LTP (see **Figure 6**). The simplest interpretation of these results is the assumption that a single activation of mGluRs is required to trigger LTP, and that their subsequent reactivation is not necessary. However, **maximal** LTP requires several bursts of NMDA activation. In other words, it seems that mGluRs provide a metabolic switch, obligatory for the induction of potentiation. This switch may be truned off by prolonged low-frequeny stimulation, which causes synapses to revert to a "de-conditioned state" in which MCPG would block LTP induction.

These experiments have also shown that the de-conditioning itself was blocked by MCPG and thus was MCPG dependent! Hence, the metabolic switch required for turning LTP on and off

would be controlled/mediated by metabotropic glutamate receptors, although by different subtypes. "Turning on" switch, kept in the off position by kinase inhibitors, is consistent with the proposition that the actual signal transduction pathway proceeds *via* PKC and subsequent phosphorylation.

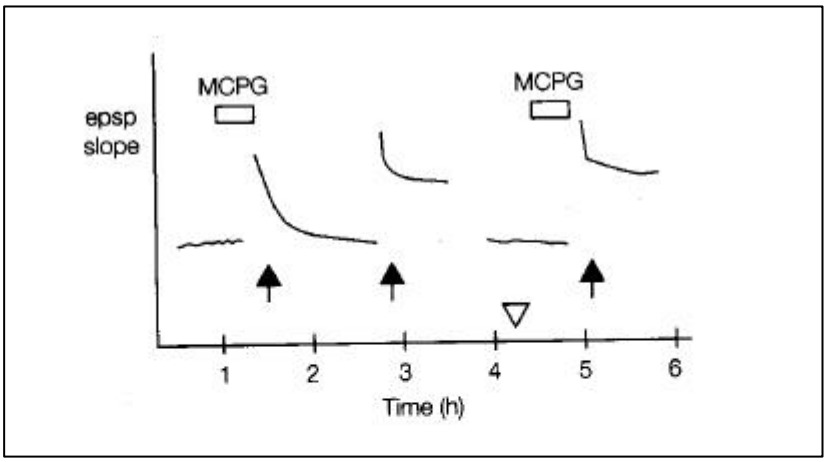

Figure 6: Evidence of conditioning by mGluRs. The first tetanic stimulus in the presence of MCPG produces only a short-term potentiation but no LTP. The second tetanic stimulus after the drug has been washed out produces LTP. At "open triangle" point, the strength of the single stimulus used to test the preparation is reduced so as to restore the baseline. A third tetanic stimulation evokes further LTP even in the presence of MCPG (Bortolotto *et al*., 1994).

1.4 Presynaptic LTP and role of retrograde messengers

Not all the authors agree on the mechanism of LTP expression. As in many other areas of research, two major groups can be identified, advocating opposite points of view. The issue of argumentation is whether LTP expression is pre- or postsynaptic? Is the enhancement in synaptic transmission due to an increase in neurotransmitter release? And, if so, which kind of signal is delivering the message to presynaptic cell, that next time more glutamate should be released? A current idea is that a diffusible second messenger, generated postsynaptically, crosses the synaptic cleft in the "wrong" direction and, arriving at the presynaptic bouton, alters release properties. Several candidates have been proposed for such a **retrograde messenger** (see below). The concept of a presynaptic component in LTP implies enhanced activation of both AMPA and NMDA receptors, since both receptor subtypes would be exposed to increased glutamate concentration. This has been confirmed, with the AMPA component being potentiated to a greater extent than the NMDA one.

Various approaches have been tried out in order to demonstrate increased transmitter release, including:

- depolarisation-evoked release of radiolabeled glutamate from synaptosomes of hippocampal slices following LTP induction *in vivo* or *in vitro* (Lynch *et al.*, 1989);
- measuring extracellular glutamate concentrations during LTP using glutamate-sensitive electrodes or outside-out patches containing glutamate receptors (Jay *et al.*, 1999);
- quantal analysis of neurotransmitter release (Voronin, 1994).

None of these strategies so far has offered solid support for increased glutamate release, but several candidates for retrograde messengers have been identified. They include platelet-activated factor (PAF) (Bazan, 1998), arachidonic acid (Williams *et al.*, 1989) and nitric oxide (NO) (Kendrick *et al.*, 1997). All of them have been shown to induce LTP, but none of them seems to be a necessary component in LTP induction. Nitric oxide, the most investigated retrograde messenger candidate[2], is also a source of big controversies, since mice lacking NO synthase have been shown to have both normal and impaired LTP. Reports from Eric Kandel's group suggest that the properties of the two subtypes of this enzyme (endothelial and neuronal) have to be taken into account, as well as their distribution throughout the hippocampus (O'Dell *et al.*, 1994; Son *et al.*, 1996).

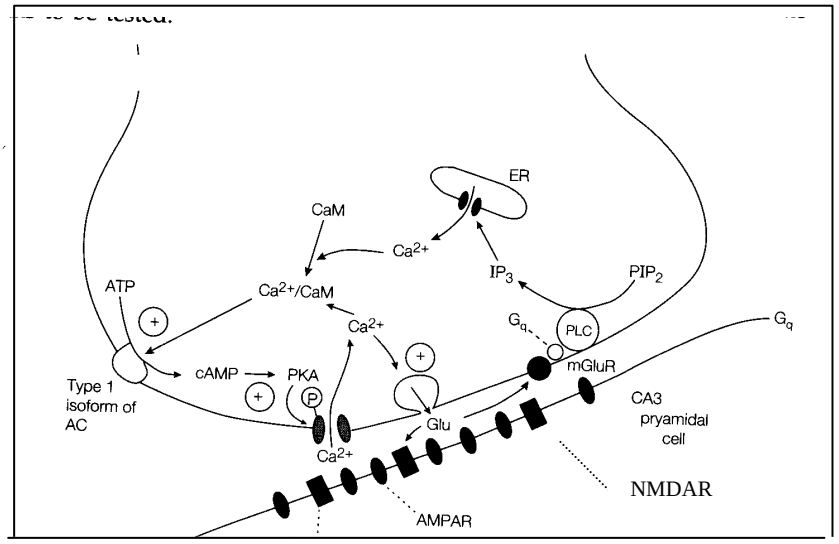

Figure 7. Mossy fiber – CA3 LTP is probably presynaptic (Revest and Longstaff, 1998).

[2] "NO AND LTP" yielded 633 hits in MEDLINE search on October 29th 2000, compared to 12 and 40 for "PAF AND LTP" and "arachidonic AND LTP", respectively.

In one particular case, the mossy fiber-CA3 synapses, it is well elaborated that LTP proceeds by a presynaptic mechanism: LTP induced there is insensitive to the NMDAR antagonist AP5, and it cannot be prevented by postsynaptic injection of calcium chelators. Neither can its induction be achieved by postsynaptic depolarisation. Mechanism of this LTP therefore most probably proceeds *via* activation of mGluR1 at the presynaptic membrane (Son and Carpenter, 1996). Calcium, released from presynapic endoplasmic reticulum, may bind to calmodulin, which in turn binds to adenylate cyclase (isoform 1). Increased levels of cAMP could then trigger PKA to phosphorylate P-type voltage-gated calcium channels, thus increasing their permeability and, consequently, glutamate release (**Figure 7**).

1.5 *Calcium imaging and LTP*

Calcium ions play a pivotal role in the induction of long-term potentiation, and more than a dozen of sensitive, fluorescent, cell-permeable dyes are available to record the change in intracellular Ca^{2+} level (Hougland, 1999).Therefore, it is possible to follow such changes by means of fluorescence microscopy. Research on LTP done by calcium imaging has been performed by both confocal laser scanning and "normal" fluorescence microscopy (*e.g.* Hansel *et al*., 1997; Wu and Saggau, 1994; Abe and Saito, 1992; Tekkök *et al.*, 1999).
One of the most popular calcium-sensitive dyes is fura-2 (Poenie and Tsien, 1986) (for the full name, see the **List of Abbreviations)**. **Figure 8** depicts its chemical structure.

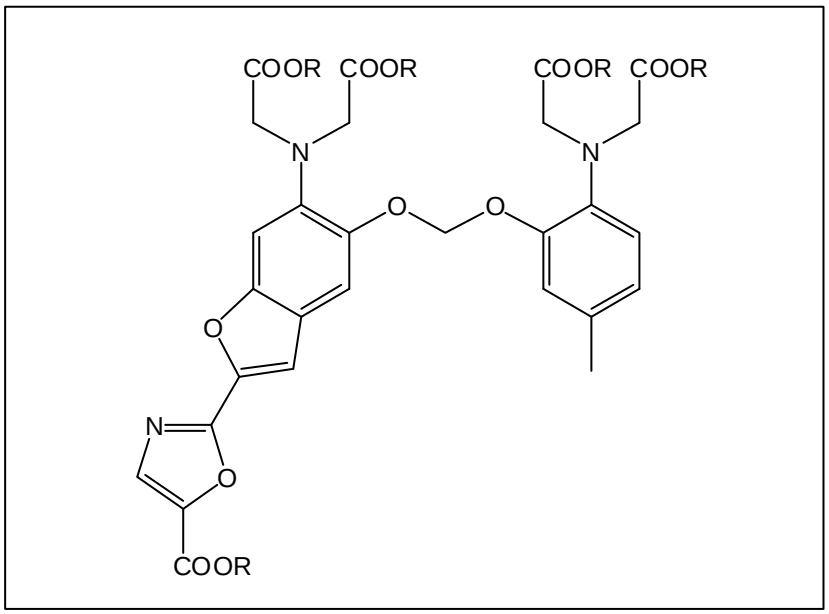

Figure 8. Structural formula of fura-2. (R = CH_2OCOCH_3, H)

Fura-2 is a UV-excitable dye, absorbing the light in the higher UV region (approx. 250 – 400 nm). The emission maximum is at 510 nm (**Figure 9**).

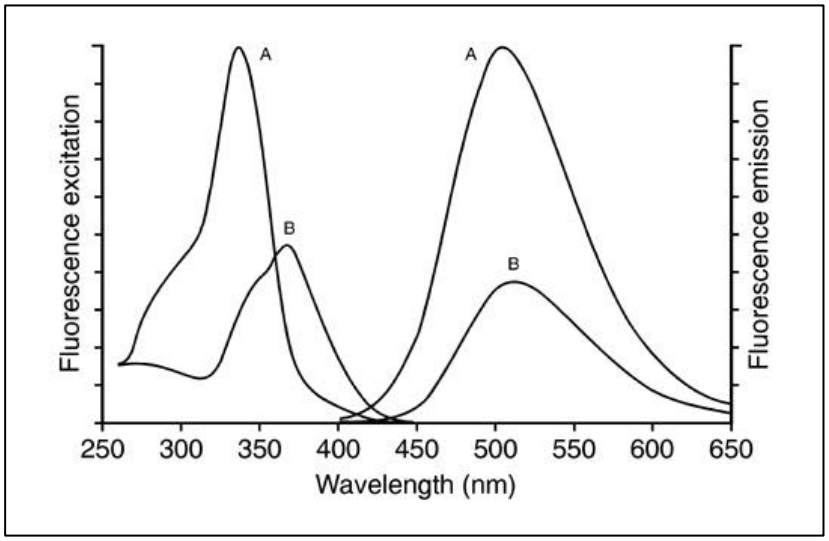

Figure 9. Fluorescence excitation (the emission detected at 510 nm) and emission (excited at 340 nm) spectra of Ca^{2+}-saturated (A) and Ca^{2+}-free (B) fura-2 in pH 7.2 buffer (copied from www.probes.com, Molecular Probes Inc.)

Upon biding to calcium ion, fura-2 changes its fluorescence spectrum, shifting the excitation maximum from 380 to 340 nm. Therefore, formation of the [fura-2-Ca^{2+}] complex (in equimolar stoichiometry, since calcium's coordination number is 8) could be registered either as an increase or a decrease in fluorescence intensity, excited by 340 and 380 nm, respectively. The most important consequence of this "dual excitability" is a possibility to avoid the influence of dye bleaching on the data acquired, since the loss in fluorescence intensities at 340 and 380 nm does not affect the intensity ratio (I_{340}/I_{380}). Ratio values are proportional to calcium concentration, and there are several methods of its calibration (**Materials and Methods**, p. 40; **Results**, p. 15; **Discussion**, p. 44).

1.6 An application example

Alzheimer's disease (AD) is the most common form of dementia among the aged population. It manifests as a progressive loss of memory (particularly recent one) and other cognitive functions. Hallucination, confusion, aggression, depression and Parkinsonism also occur in some, but not all patients (Alberca *et al.*, 2000). Death occurs after 3-15 years, and incidence of the disease by people over 80 is more than 20% (Hoyert and Rosenberg, 1997: Hoyert and Rosenberg, 1999; Witthaus *et al.*, 1999).

These symptoms correlate to a large loss of neurons, in both cortical and subcortical brain regions (West et al., 1994; Hof *et al*., 1990 (a); Hof *et al*., 1990 (b)). Brain weight is reduced by 30-40% (Riederer and Jellinger, 1982). In many patients, there is a large reduction in cortical activity of the marker for cholinergic neurons, choline acetytransferase (Katzman *et al.*, 1988).

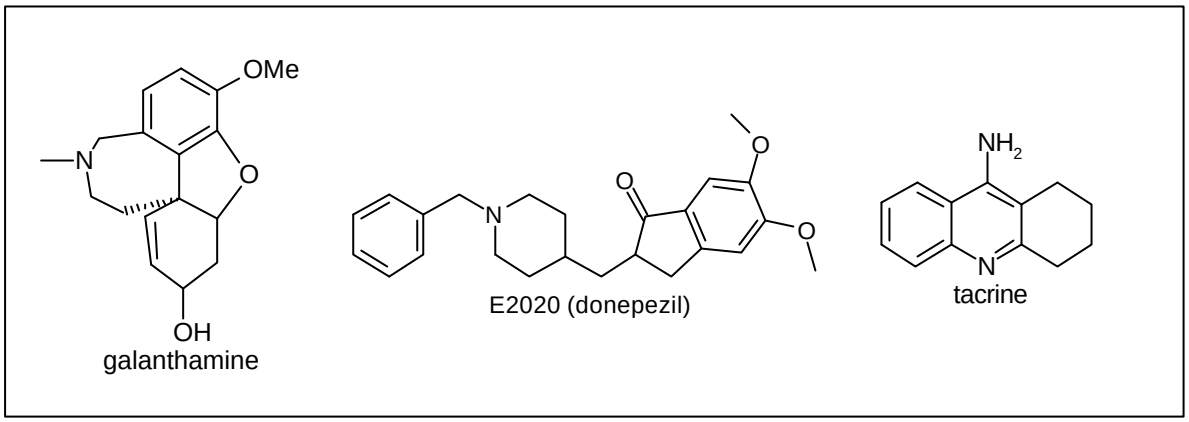

Figure 10. AchE blockers, approved anti-AD drugs.

This loss of cholinergic neurons is what underlies the rationale for use of the only three drugs licensed for the AD treatment: tacrine (Qizilbash *et al*., 2000), E2020 (donepezil) (Birks and Melzer, 2000) and galanthamine (Fulton and Benfield, 1996) (**Figure 10**). All of them are non-covalent blockers of acetylcholine esterase (AchE), whereas galanthamine - as earlier studies from our group have demonstrated (*e.g*. Schrattenholz *et al.*, 1996) - shows another interesting feature: it modulates nAChR currents, by binding to an allosterical site of the receptor.

Nicotinic acetylcholine receptors have been shown to play a significant role in LTP modulation, since nicotine treatment affects hippocampal long-term potentiation (Chen and Chen, 1999; Hunter *et al.*, 1994; Sawada *et al.*, 1994). In addition, nicotine is a well-known memory enhancer in *in vivo* studies (Arendash *et al.*, 1995; Radcliffe and Dani, 1998; Gamberino and Gold, 1999), and its consumption by smoking (*i.e.* chronical exposure) negatively correlates to incidence of developing Alzheimer's disease (van Dujin and Hofman, 1991).

The cholinergic system is not the only one that becomes seriously damaged by Alzheimer's disease. Glutamatergic neurons also belong to this group (Nordberg, 1992). Inter-relations between plasticity, memory, memory loss, glutamate, acetylcholine and calcium (nAChRs are ion channels, permissive to calcium ions as well) were reasons for deciding to test the influence of nicotine and galanthamine on the Ca^{2+} influx changes, using our experimental model (see **Results**, p. 33, and **Discussion**, p 51).

1.7 AIM OF THE WORK

The main objective of this work was to demonstrate that long-term potentiation (LTP) can be studied on a primary hippocampal cell culture, using fluorescence microscopy (calcium imaging). Such a model system would provide a set of data complementary to the electrophysiological ones, mainly concerning spatio-temporal ion dynamics in the cell or the cell region (*e.g.* dendryte or the cell body). In order to demonstrate it, typical features of electrophysiologically studied LTP had to be confirmed in our system, by measuring intracellular calcium levels. These features include:

- critical dependence on NMDARs and mGluRs, and
- relative independence on AMPARs and L-type VGCCs.

Another objective was providing an application example for the new LTP model system. In this work it was modulation of glutamate-induced potentiation by nicotine and galanthamine, an approved anti-AD drug. Rationale for choosing this application example was:

- **LTP** is the widely accepted model for learning and **memory** on the cellular/molecular level;
- **AD** patients' **memory** is severely affected by the disease, and
- **AD** is shown to damage **nicotine**rgic and **glutamate**rgic neurons in the **hippocampus**, both having been shown to play a prominent role in synaptic plasticity (**LTP/LTD**).

2. MATERIALS AND METHODS

2.1 Primary culture of hippocampal cells

Cell cultures used in this work have been made according to the modified procedure of Brewer's (Brewer, 1995). Tissue originated from 1 – 3 days old female Sprague – Dawley rats. All steps of preparation were done under sterile conditions, in a laminar flow hood. For the purpose of analysis by calcium imaging and immunofluorescence experiments, cells were cultivated on glass coverslips (d = 12 mm).

- *Preparation of the glass coverslips*

- glass coverslips (Assistent, Germany) were put into a large (d = 12 cm), sterile Petri dish (Greiner, Germany) and treated under shaking in absolute ethanol (Aldrich) for 4 h;
- ethanol was poured off, and the coverslips washed ten times with de-ionized (Millipore) water (conductance: 18.2 MΩ/cm);
- coverslips were moved on to a sheet of Whatman paper and allowed to air-dry;
- after drying, coverslips were transferred into a clean glass vessel and heat-sterilized (180 ^{o}C, 4 h);
- sterile coverslips (at room temperature) were put into wells of a 24-well cell culture plate (Grainer), one coverslip/well;
- 0.5 mL of poly-L-lysine (MW 70 – 150 kDa, Sigma) solution (50 μg/mL in water) was poured into each well – incubation with PLL lasted from 20 min to 12 h, without notable difference in quality of the cell culture;
- after incubation, coverslips were washed twice with sterile Millipore water and allowed to dry.

- *Preparation of hippocampal cells*

- animals were killed by decapitation, and the scull was opened by two lateral cuts from the spinal opening up to the ears, and by one medial cut from the spinal opening almost to the nose (paying attention not to damage the brain tissue underneath!);
- brains were transferred into ice-cold HibA solution (98.25% HibernateA medium, 1% B27 supplement, 0.25% 200 mM L-glutamine solution, 0.5 % 100x penicillin-streptomycin solution, all Gibco);

- hippocampi were isolated by excising ith a scalpel the bulbi olfactorii and the cerebellum, than dividing the remaining dien- and telencephalon longitudinally into two symetrical, lateral halves, removing (by forceps) the basal ganglia that mask the hippocampus and finally excising/isolating it, either by using two forceps or, alternatively, one forceps and a fine scissors (**Figure 11**);

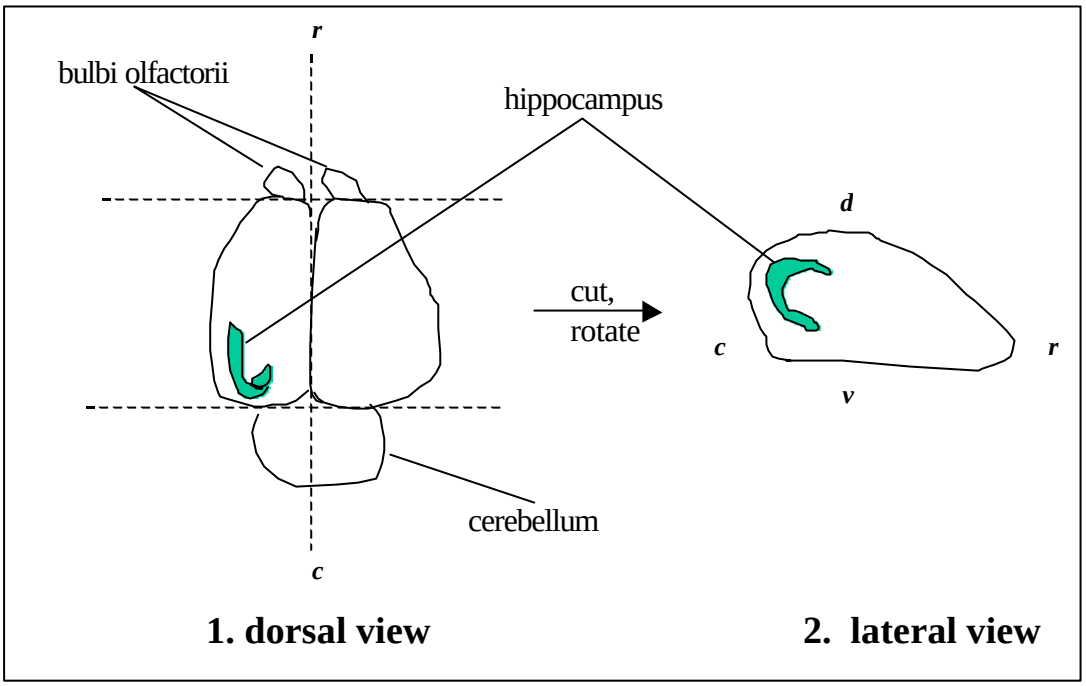

Figure 11. Scheme of hippocamus isolation. Only one of the hippocampi is shown for clarity. Dashed lines represent the excision routes. (*r, c, d, v*: rostral, caudal, dorsal, ventral)

- after isolation, the meningae and larger blood vessels were removed, and the tissue was cut (transversely to its longitudinal axis) into approx. 500 µm thick slices;
- slices were transferred – using a gentle brush - into tubes with 2 mL of papain-containing (20 U/mL, Sigma) HibA solution (4 hippocampi per tube);
- these tubes, occasionally shaken, were let to stay for 20 – 40 min in 37 ^{o}C water bath;
- with the fire-polished, air-cold Pasteur pipette (tip diameter approx. 1 mm), tissue pieces were moved into fresh HibA solution (1, 5 mL) at the room temperature, each fresh portion corresponding to the one papain-containing tube;
- tissue pieces were triturated by the Pasteur pipette, untill the cells (approx. 5 – 7 in-and-out cycles) were properly dissociated;
- this suspension was allowed to settle (5 – 10 min), tissue pieces from the bottom of the tube were moved into fresh HibA solution and re-triturated to completion;
- the resulting cell suspensions were combined into two tubes, and centrifuged for 6 min at 1000 rpm;

- the pellet (cells) was twice resuspended and washed with 2 mL of fresh HibA solution;
- after a second washing, cells were resuspended into 2 mL/tube NeurobasalA solution (98.25% NeurobasalA medium, 1% B27 supplement, 0.25% 200 mM L-Gln solution, 0.5 % 100X penicillin-streptomycin solution, all Gibco), and combined into a single tube, containing finally 4 mL of the cell suspension.

- *Cell counting and plating*

- 10 µL of the cell suspension was mixed with 30 µL of trypan blue solution (1:4 dilution), producing the suspension of which an aliquot was filled into the Neubauer cell counting chamber;
- the number of cells (N) was counted from four big squares (V = 10^{-4} mL each) and was used to calculate the total yield (Y) of the preparation: Y = N*4*10^4 (4 is the correction factor for the trypan blue dilution, and the initial volume of the cell suspension (4 mL) is equal with the number of big squares, used for counting);
- typically, Y of approx. 7,500,000 cells from 12 hippocampi was obtained and used to make 18 mL of cell suspension ($\rho \cong 420{,}000$ cells/mL), which was plated on 36 PLL-coated glass coverslips (0.5 mL/well, approx. 110,000 cells/cm^2);
- the cell culture plates were put into an incubator (37 ^oC, 5% CO_2) for 60 min, and the coverslips were quickly moved into wells with fresh NeurobasalA solution;
- medium was exchanged once a week, by removing approx. 1/3 of the volume and adding 250 µL of the fresh one;
- cells were cultured from two to four weeks.

2.2 Calcium imaging experiments

- *Fura-2 loading procedure (Haugland, 1999)*

- Fluorescent dye Fura-2 AM (Molecular Probes, Leiden, The Netherlands) stock solutions (1 mM) were prepared in dry DMSO;
- **c**ells were loaded with the fura-2 AM by transferring the glass coverslips into Neurobasal A medium, containing 2 µM fura-2 AM;
- after incubating for 40 min at 37 ^0C at 90% O_2 and 10% CO_2, the coverslips were moved to the dye-free medium, and additional 30 min were allowed to end the dye deesterification.

- *Acquiring fluorescent images (Abe and Saito, 1992)*

- after deesterification, coverslips were fixed (using silicone grease) to the recording chamber, which was then mounted onto the stage of an inverted light microscope (Axiovert 100, ZEISS, Germany), equipped with a UV-illumination source (75W XBO lamp, OSRAM, Germany) and a 40x objective, numerical aperture 0.75;
- Fura-2 fluorescence was recorded by using excitation wavelengths of 340 (λ_1) and 380 (λ_2) nm, and emission wavelength of 510 nm;
- images were acquired by cooled (- 25 ^{o}C) CCD-camera (Princeton Instruments), having 680 x 480 resolution with a pixel size of 6.8 x 6.8 μm;
- wavelength and illumination control were obtained by appropriate (340 and 380 nm) filters and a shutter (speed: 20 ms), controlled by Ludl MAC 2000 Controller;
- illuminations at 340 and 380 nm lasted 500-700 and 120-150 ms, respectively;

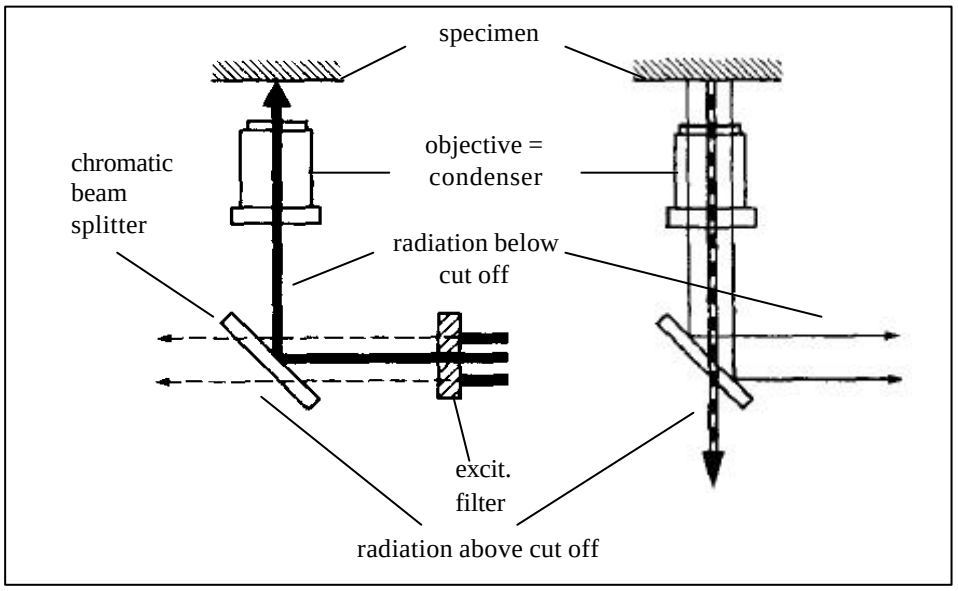

Figure 12. Scheme of the optical apparatus.

- acquisition and analysis of the data were performed by using MetaFluor 2.0 software (Universal Imaging Corporation);
- regions chosen to analyse were bodies of the cells identified as neurons (see **Results**, **Figure 19**, immunostaining);
- instrument was calibrated by the equation calibration method, described by Poenie *et al.* in 1986 [$(Ca^{2+})_i = K_d(F_{min}/F_{max})(R\text{-}VR_{min})/(VR_{max}\text{-}R)$];

- $(Ca^{2+})_0$ and $(Ca^{2+})_{max}$ solutions were obtained from Molecular Probes. (Kd = 224 nM, F_{min}/F_{max} and R_{min}/R_{max} represent λ_2- and ratio-image intensities at zero and saturating (Ca^{2+}), respectively. *V* is viscosity factor).

- *Stimulation of the cells*

- if not stated otherwise, every group of cells was stimulated twice for 30 s each (one pair of images being acquired every five seconds), with 35 min intermission between the applications (Malgaroli and Tsien, 1992);
- stimulation buffer (SB) for the Ca^{2+}-imaging experiments contained, in mM: 125 NaCl, 5 KCl, 6 $CaCl_2$, 0.8 $MgCl_2$, 5 glucose, 20 HEPES (pH 7.3), and was added (in μM) 50 L-glutamate, 10 glycine and 10 bicuculline;
- in blocking/modulation experiments, SB was added (in mM) 25 AP-5 (NMDAR antagonist), 10 CNQX (AMPAR antagonist), 500 (S)-MCPG (mGluR antagonist), 10 nifedipine (L-type VGCC antagonist), 100 nicotine (nAChR agonist), 0.5 galanthamine and 0.5 rivastigmine (AChE blockers), as explained in the **Results**;
- composition of the washing buffer (WB) was (in mM): 125 NaCl, 5 KCl, 2 KH_2PO_4, 2 $CaCl_2$, 1 $MgCl_2$, 5 glucose, 20 HEPES (pH 7.3);
- washing was performed by gravity-fed perfusion system (**Figure 13**);
- HEPES, NaCl, KCl, $CaCl_2$, $MgCl_2$, L-glutamate, glycine, nicotine and glucose were obtained from Sigma;
- AP-5, CNQX, MCPG, bicuculline and nifedipine were provided by BioTrend, Germany;
- galanthamine and rivastigmine were provided by Janssen Research Foundation, Beerse, Belgium.

- *Data analysis*

- during each stimulation (duration: 30s), six 340/380 nm image pairs were acquired (except in the experiment depicted by the **Figure 23**);
- regions of the cells were selected (neuronal cell bodies) for ratio calculation;
- ratio values derived from the first image pairs taken during the stimulation were taken as representative for a given condition;
- ratio values (corresponding to $[Ca^{2+}]_i$) in cells prior to stimulation were subtracted from the values after stimulation, thus giving ratio increase (ΔR);

- the resulting ΔR values were compared to ΔR values from other stimulation events;
- significance of difference between the mean subtracted values was determined either by independent two-population t-tests (0.05 level - error bars in all the graphs correspond to standard errors of mean) or by non-parametric tests (Kruskal-Wallis tests) (Motulsky, 1995);
- statistical significance for the cases where $0.05 > p > 0.01$, $0.01 > p > 0.001$ and $0.001 > p$ were marked by "*", "**" and "***", respectively;
- case where no statistical significance could be stated ($p > 0.05$) were marked by "n.s.".

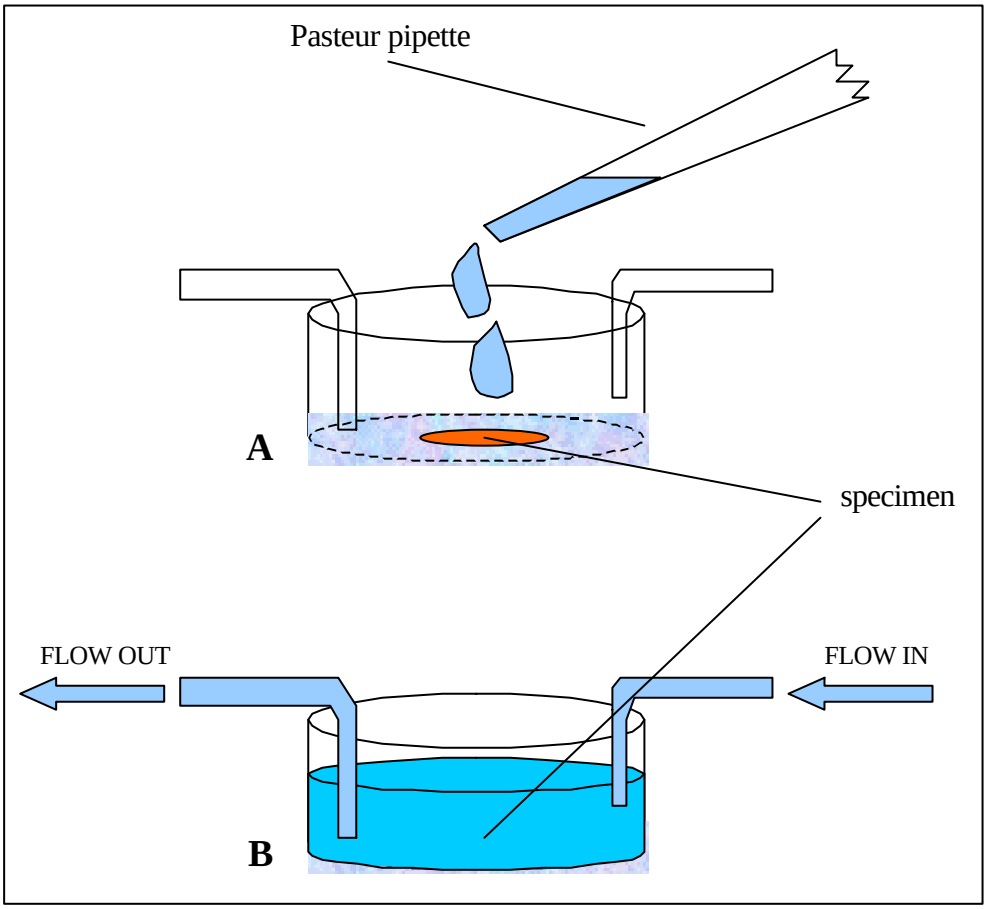

Figure 13. Schematic drawing of the stimulation and washing apparatus. Flow-in and flow-out were gravity-fed. Stimulating solution was applied drop-wise onto the coverslip carrying the cells.

2.3 Immunocytochemistry

Primary hippocampal neurons were labelled by means of indirect immunofluorescence technique, which utilises primary (cell-specific) and secondary (primary antibody-specific) antibodies. The primary antibody used in these experiments was directed against α-Tau protein (IgG, rabbit, polyclonal), diluted 1:100. The secondary antibody (goat, IgG, anti-

rabbit, Texas Red-coupled, Jackson Research) was diluted 1:200. Antibody dilutions were made in dilution buffer (DB): 10% fetal calf serum (FCS), 0.02% Sodium azid in phosphate-buffered saline.

- cells have been fixed for 15 – 20 min in 4% solution of *p*-formaldehyde in PBS, and washed for 10 min in PBS alone (3 buffer exchanges);
- cell membranes have been perforated by 0.5% solution of Triton X-100 in PBS (10 min, RT);
- washing: 1 x 5 min, in PBS;
- incubation with the primary antibody, 30 min at RT, inside of a moist compartment;
- washing: 3 x 5 min, in PBS;
- incubation with the second antibody, 30 min at RT in the dark, inside of a moist compartment;
- washing: 3 x 5min, in PBS;
- cells have been covered by covering solution (1mg/ml *p*-phenylendiamine in PBS, 30% glycerine, 100 mg/ml elvanol; pH 8.5, prepared from the aliquotes kept at -20°C), in a way that a drop of the solution has been applied onto an object glass and the coverslip with the cells has been put into it (cells facing the drop);
- to protect the samples form drying out, coverslips have been covered with a film of nail enamel and kept at –20 ^{0}C;
- fluorescent images have been taken using Zeiss upright microscope.

3. RESULTS

3. 1. Description of the system used for biochemical studies of LTP

Prior to performing experiments that could establish quantitative correlation between changes in calcium influx and various components of glutamatergic neurotransmission in primary culture of hippocampal cells, the following basic information about the system needed to be obtained:

a) appropriate glutamate concentration for LTP induction;
b) analysis of effects of fura-2 AM concentration on the glutamate-induced potentiation;
c) analysis whether glutamate stimulation under our conditions induces excitotoxicity;
d) analysis of "contaminating" effects, due to the presence of glial cells.

- *Appropriate glutamate concentration for LTP induction*

An important step in finding optimal conditions for the chemical induction of LTP was to determine the relationship between glutamate concentration applied and the calcium influx produced. To obtain these data, a set of cells was exposed to subsequent applications of 0.5, 2, 5, 10, 20, 50 and 100 μM of L-glutamate (**Figure 14, Table 1**). Each application lasted 15 seconds, with a 20 min intermission between each of them[1]. These data were fitted with a one-site binding sigmoidal curve model, with an apparent EC_{50} of 5.6 ± 0.3 μM. This value is similar to those previously reported for glutamate and hippocampal neurons (*e.g.* EC_{50} = 2.3 μM: an electrophysiological study by Patneau and Mayer, 1990), but it is noteworthy to mention that it might be influenced by the very property that we wanted to determine, *i.e.* by **time-dependent, glutamate-evoked changes in calcium influx**. To test this possibility, another, glutamate-untreated group of neurons was given a 50 μM Glu stimulus, and the calcium influx (**Figure 15**) for this concentration under both paradigms was compared.

[1] Fifteen seconds of stimulation was the minimal time that could be used with our application system (see **Materials and Methods**). Twenty minutes of intermission was enough for all cells to return to the basal state.

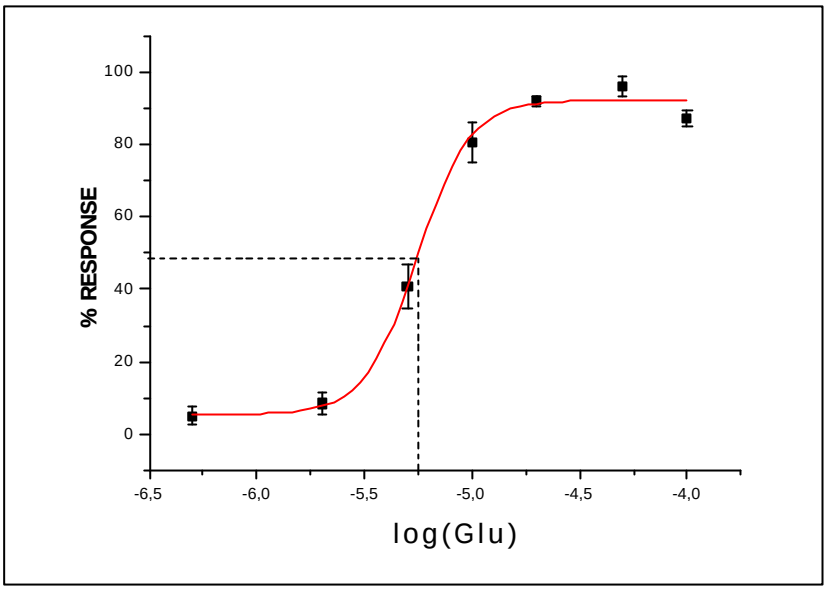

Figure 14. Glutamate dose-response curve, obtained with pre-stimulation. The signals were recorded from a group of cells, stimulated by increasing concentrations of glutamate (0.5, 2, 5, 10, 20, 50 and 100 mM). The stimuli lasted 15 s each, and were separated by 20 min long intermissions. Number of the cells was 17. EC_{50} = 5.6 ± 0.3 mM. Error bars are s.e.m.

Glu (mM)	Norm. resp. (%)	s.d.	s.e.m.	N
0.5	5.047	10.488	2.543	17
2	8.542	13.249	3.213	17
5	40.705	24.685	5.987	17
10	80.389	22.751	5.518	17
20	91.871	4.916	1.192	17
50	96.065	11.245	2.727	17
100	87.173	9.615	2.332	17

Table 1. Data fitted into the dose-response curve (Fig. 14). Response was normalized against the cell with the largest calcium influx. Number of cells: 17. Number of experiments: 1. (s.d. and s.e.m. are standard deviation and standard error of mean, respectively.)

As can be concluded from **Figures 14, 15** and **Tables 1, 2**, responses evoked by 50 µM glutamate are significantly larger if cells were not pre-treated with a series of glutamate stimuli. Therefore, in order to test the possibility that cells without prior stimulation might have significantly different dose-response curve parameters, an experiment was performed where each glutamate concentration was applied onto previously non-stimulated group of neurons (**Figure 16, Table 3**).

Two-population t-test at 0.05 level: t = -5.384 p = 7.821 x 10^{-7}
At the 0.05 level, the two means are significantly different.

Prestimulation	Mean	s.d.	s.e.m.	N	Stat. sig.
without	219.575	87.578	11.213	61	***
with	100	48.832	11.843	17	-

Table 2. Statistical comparison of the responses to 50 mM glutamate taken from the dose-response curve (Fig. 14) and the responses of previously non-stimulated cells. Mean intensity of the 50 mM response from the dose-response curve was taken to be 100.

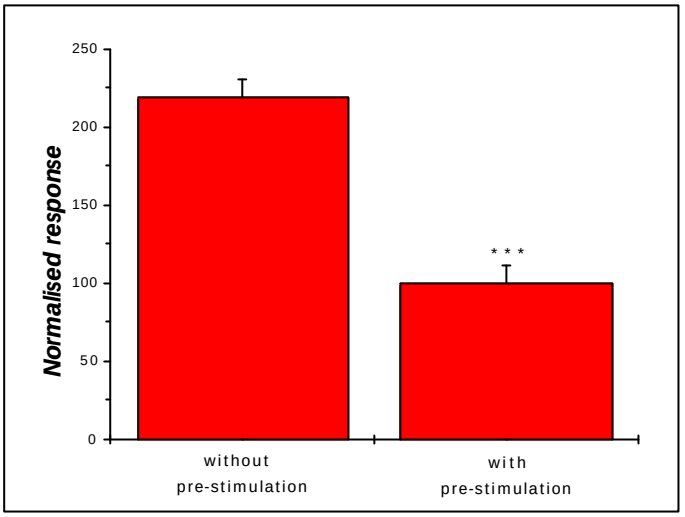

Figure 15. Response to 50 mM Glu is significantly smaller if the cells were previously stimulated, suggesting that previous condition influences later responses. The column "without pre-stimulation" represents the normalized ratio increase (DR) after the cells were stimulated with glutamate for the first time. The column "with prestimulation" corresponds to the DR value where the cells were already treated with 0.5, 2, 5, 10 and 20 mM Glu before the 50 mM Glu stimulus was applied. Number of cells with and without prestimulation was 17and 61, respectively. Error bars are s.e.m.

The prestimulation-unaffected dose-response curve has been made by applying given glutamate concentration to a sample of untreated cells. This method, however, is of much lower accuracy because of unavoidable differences between the cell samples. The curve obtained by such an approach (**Figure 16, Table 3**) results in larger EC_{50} value of 18 ± 5 µM.

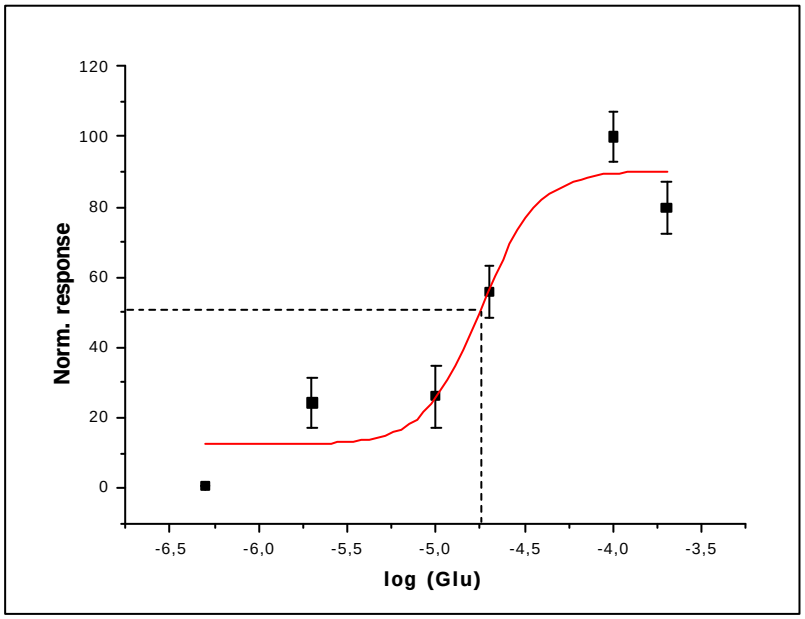

Figure 16. Glutamate dose – response curve, obtained without pre-stimulation. Responses to various glutamate concentrations (0.5, 2, 10, 20, 100, 200 mM) were recorded each from a different sample of previously non-stimulated cells. EC_{50} = 18 ± 5 mM. Number of experiments: 1. Number of cells per concentration varied from 17 to 31. Error bars are s.e.m.

Glu (mM)	Norm. resp. (%)	s.d.	s.e.m.	N
0.5	0.552	0.6714	0.137	24
2	24.189	29.188	7.079	17
10	26.190	37.351	8.803	18
20	55.877	36.168	7.233	25
100	100	39.550	7.103	31
200	79.894	38.341	7.378	27

Table 3. Data fitted into the dose-response curve (Fig. 16). Response was normalized against the sample with the largest mean calcium influx. Number of experiments: 1. (s.d. and s.e.m. are standard deviation and standard error of mean, respectively.)

In order to select an optimal concentration for our system, we referred to the available literature and the data from our dose-response curves. In 1992, Malgaroli and Tsien described a successful attempt of LTP induction in primary culture of hippocampal cells, by appplying 50 µM glutamate for 30s. We tried 50 and 100 µM glutamate stimuli, since both of them were able to elicit strong responses (**Figs. 14** and **16**). The experimental paradigm for LTP induction and detection – as already explained – consisted of two subsequent glutamate applications on the same group of cells, with a 35 min intermission between them. Responses evoked by the stimuli were then compared, the first being subtracted from the second. The time of 35 min lies within the boundaries attributed to early-phase LTP (Huang and Kandel, 1994). **Figures 17, 18** and **19** shows how these two concentrations affected changes in calcium influx:

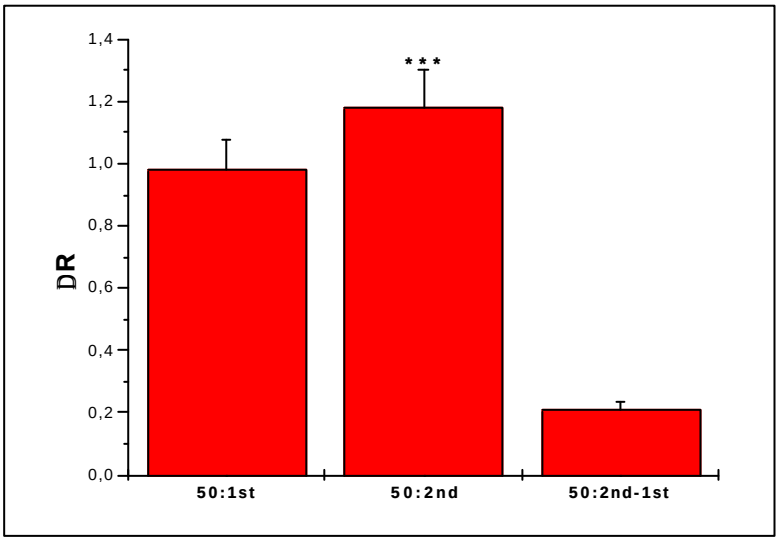

Figure 17. Glutamate application (50 mM, 30s) induces potentiation of calcium influx in the hippocampal neurons, since the second response to 50 mM glutamate (50:2nd) is larger than the first one (50:1st). Cell response corresponds to increase in fluorescence intensity ratio ($R = I_{340}/I_{380}$). This increase represents difference (ΔR) between R-values before (R_b) and during (R_s) the stimulation. Number of the cells: 17. Percentage of de- and potentiated cells was 11.8 and 88.2, respectively. Error bars are s. e. m.

Two-population t-test at 0.05 level (50:1st *vs.* 50:2nd) t = -6.937 p = 3.347 x 10^{-6}
At the 0.05 level, the two means are significantly different.

Glu (mM)	Mean	s.d.	s.e.m.	N	Stat. Sig.
50:1st	0.978	0.399	0.097	17	-
50:2nd	1.184	0.484	0.117	17	***
50:2nd-1st	0.206	0.122	0.030	17	-

Table 4. Glutamate stimulus of 50 mM induces calcium influx potentiation. Potentiation is defined as difference in response (*i.e.* ratio increase) ($DR_2 - DR_1$) between the second and the first stimulation. Number of experiments: 1.

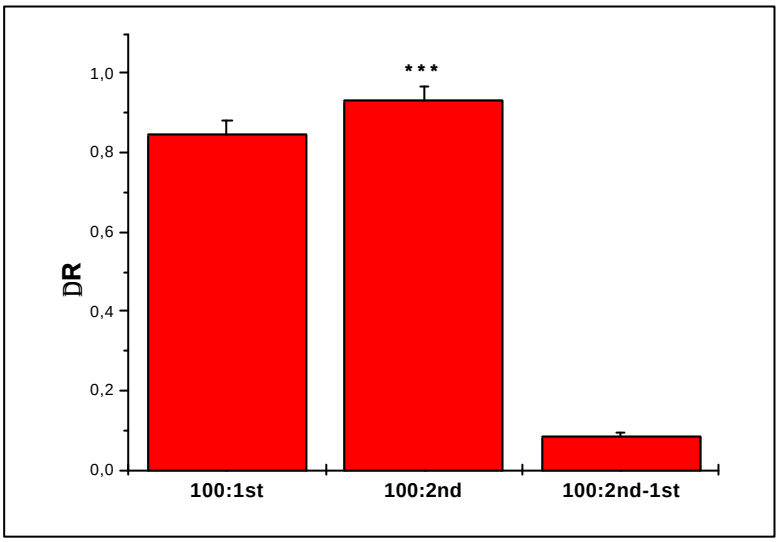

Figure 18. Glutamate application (100 mM, 30s) induces potentiation of calcium influx in the hippocampal neurons, since the second response to 100 mM glutamate (100:2nd) is larger than the first one (100:1st). Cell response corresponds to increase in fluorescence intensity ratio ($R = I_{340}/I_{380}$). This increase represents difference (DR) between R-values before (R_b) and during (R_s) the stimulation. Number of the cells: 17. Percentage of potentiated cells was 100. Error bars are s.e.m.

Two-population t-test at 0.05 level (100:1st *vs.* 100:2nd) t = -8.221 p = 1.659 x 10^{-7}
At the 0.05 level, the two means are significantly different.

Glu (mM)	Mean	s.d.	s.e.m.	N	Stat. Sig.
100:1st	0.848	0.142	0.033	19	-
100:2nd	0.930	0.162	0.037	19	***
100:2nd-1st	0.082	0.044	0.010	19	-

Table 5. Glutamate stimulus of 100 mM induces calcium influx potentiation. Potentiation is defined as difference in response (*i.e.* ratio increase) ($DR_2 - DR_1$) between the second and the first stimulation. Number of experiments: 1.

Additionally, it can be seen that 50 μM Glu application induces larger potentiation than the 100 μM one (**Figure 19**).

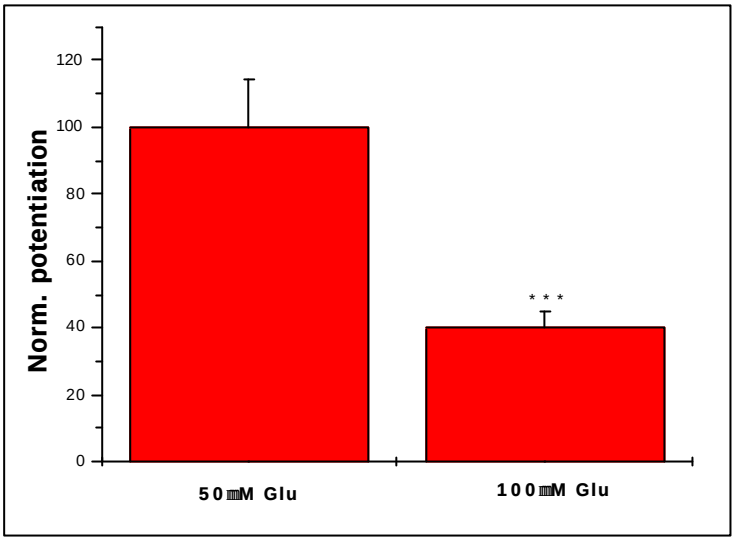

Figure 19. Application of 50 mM glutamate stimulus induces larger potentiation than the 100 mM one. Potentiation is defined as the difference in response (*i.e.* ratio increase) ($DR_2 - DR_1$) between the second and the first stimulation. Data were normalized against the mean potentiation induced by 50 mM glutamate. Number of cells was 17 (50 mM) and 19 (100 mM). Duration of each stimulus: 30s. Number of experiments: 1. Error bars represent standard error of mean.

Two-population t-test at 0.05 level: $t = -4.123$ $p = 2.273 \times 10^{-7}$
At the 0.05 level, the two means are significantly different.

Glu (mM)	Mean	s.d.	s.e.m.	N	Stat. Sig.
50	100	59.438	14.416	17	-
100	39.995	21.207	4.865	19	***

Table 6. A 50 mM glutamate stimulus induces larger potentiation than the 100 mM one. Potentiation is defined as difference in response (*i.e.* ratio increase) ($DR_1 - DR_2$) between the second and the first stimulation. Data were normalized against the mean potentiation induced by 50 mM glutamate. Number of experiments: 1.

These introductory experiments suggested that stimulation by glutamate induces changes in cell responsiveness to forthcoming stimuli: EC_{50} values determined by two approaches – with and without prestimulation - differ significantly (5.6 ± 0.3 µM *vs.* 18 ± 5 µM: see **Figures 14, 15, 16** and **Tables 1, 2, 3**) *and* glutamate application potentiates calcium influx into the neurons (**Figures 17, 18, 19** and **Tables 4, 5, 6**).

Based on these data, 50 µM Glu was selected to be our concentration of choice in looking for further similarities between our paradigm and classical LTP induction scheme. Smaller concentrations were not tested, since 50 µM Glu is expected to elicit maximal Ca^{2+} influx (Figure 16), thus providing better signal (higher signal/noise ratio).

- *Analysis of fura-2 AM concentration effects on the glutamate-induced potentiation*

As already described in the **Introduction**, plasticity-related phenomena (*i.e.* LTP and LTP) are triggered by calcium influx into the cells. For the purpose of following such phenomena directly, *i.e.* by measuring Ca^{2+} levels using fluorescence microscopy, it must be excluded that the very process of measurement affects the data themselves. In other words, the amount of calcium ions chelated by fura-2 must not be too large to deprive the LTP-inducing pathways of its *spiritus movens*. We already demonstrated that hippocampal neurons, if stimulated by 50 and 100 μM glutamate, respectively, show increased responsiveness to a second stimulation of the same kind (**Figures 17** and **18**). Both of these cell samples were diffusion-loaded in a solution containing 2 μM fura-2 AM (recommended concentrations are between 1 and 10 μM: see Haugland, 1999)[1]. To test whether higher fura-2 AM concentrations affect the measurements, we tested the influence of 50 μM glutamate stimulation on the two groups of cells, incubated in 2 and 20 μM fura-2 AM. As shown in **Figure 19**, ten times more dye in the incubation solution correlates with smaller potentiation effects, which prompted us to perform all further experiments with 2 μM fura-2 AM. Furthermore, calcium signal upon *first* stimulation is almost five times bigger when less dye is used (**Figure 20**, **Table 8**).

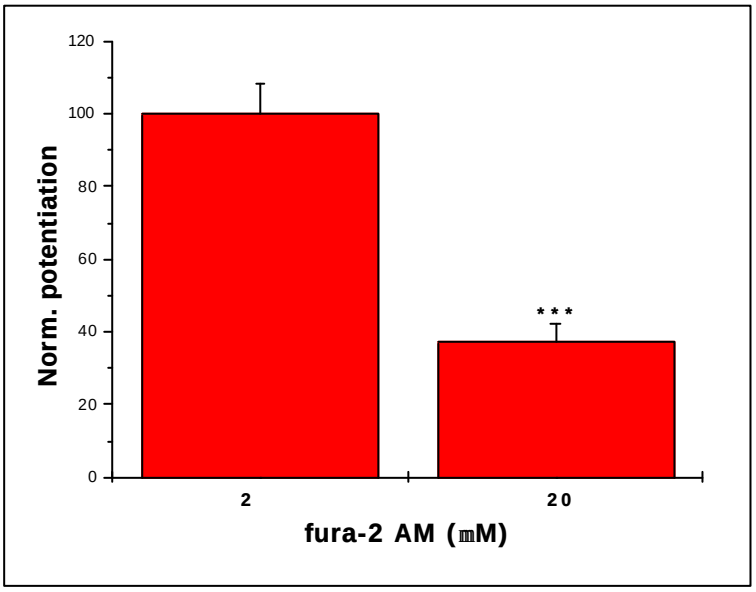

Figure 20. Concentration of fura-2 AM affects 50 mM glutamate-induced potentiation. Both groups of cells were treated with 50 mM Glu for 30 s, and the stimulus was repeated after 35 min. Difference in ratio changes (*i.e.* Ca^{2+} influx) between the two stimuli (*i.e.* potentiation: $DR_2 - DR_1$) for the two cells groups ("2" and "20": cells incubated in 2 and 20 mM fura-2 AM, respectively) was calculated, and normalized for comparison. Mean potentiation of the cells incubated in 2 mM fura-2 AM was taken to be 100. Number of the cells was 57 ("2") and 63 ("20"). Number of experiments: 2. Error bars are s.e.m.

[1] In our system, incubation in 1μM fura-2 AM solution produced significantly weaker signals (data not shown).

Two-population t-test at 0.05 level: t = -6.552 p = 1.556 x 10^{-9}
At the 0.05 level, the two means are significantly different.

fura-2 AM (mM)	Mean	s.d.	s.e.m.	Sum	N	Stat. sig.
2	100	61.824	8.190	5699.985	57	-
20	37.132	42.312	5.334	2339.483	63	***

Table 7. Concentration of fura-2 AM affects 50 mM glutamate-induced potentiation. Tenfold increase of fura–2 AM amount in incubation solution correlates to 2.7-fold decrease in Ca^{2+} influx potentiation. Mean ratio change in the cells incubated in 2 mM fura-2 AM was taken to be 100. Percentage of de- and potentiated cells in "2" and "20" group was 0 and 100, and 4.8 and 85.7, respectively. Number of experiments: 2.

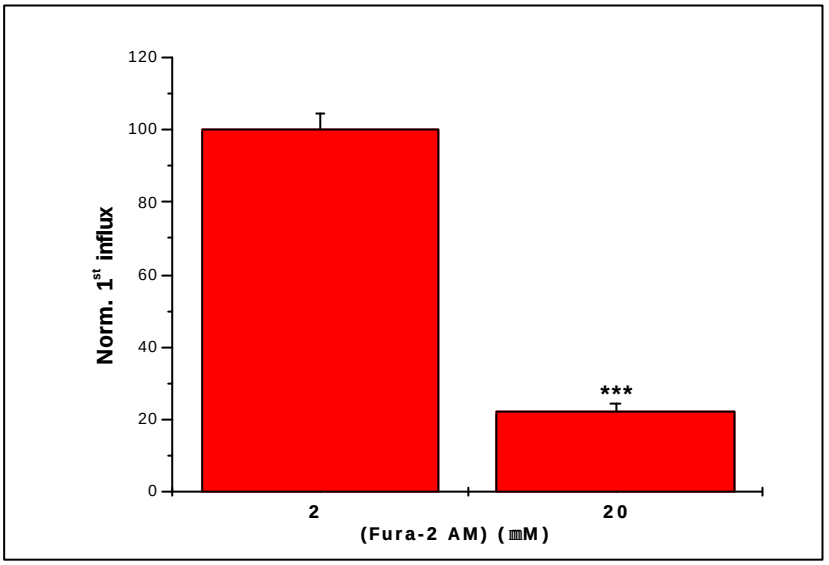

Figure 21. Cells loaded with 2 mM fura-2 AM solution (2) show nearly five times larger Ca^{2+} influx during the first stimulation than the cells loaded with 20 mM fura-2 AM solution (20). The two groups of cells were stimulated with 50 mM glutamate and the yielding increase in I_{340}/I_{380} ratio was calculated (DR = R_s – R_b: R_s and R_b are the mean ratio values in the stimulated and the basal (resting) state, respectively.) For comparison, cell responses were normalized (mean ration increase for the group incubated in 2 mM fura-2 AM was taken to be 100). Number of the cells was 57 ("2") and 63 ("20"). Number of experiments: 2. Error bars are s.e.m.

Two-population t-test at 0.05 level: t = -15.829 p = 5.809 x 10^{-31}
At the 0.05 level, the two means are significantly different.

fura-2 AM (mM)	Mean	s.d.	s.e.m.	Sum	N	Stat.
2	100	35.023	4.639	5700.019	57	-
20	22.403	16.149	2.035	1411.372	63	***

Table 8. Cells loaded with 2 mM fura-2 AM solution (2) show nearly five times larger Ca^{2+} influx during the first stimulation than the cells loaded with 20 mM fura-2 AM solution (20). For comparison, cell responses were normalized (mean ration increase for the group incubated in 2 mM fura-2 AM was taken to be 100). Number of the cells was 57 ("2") and 63 ("20"). Number of experiments: 2.

Although it would be expected that the higher fura-2 AM concentration gives rise to the higher ratio signal, there are two factors that should not be neglected in evaluating these data. Firstly, it is possible that *intracellular* concentration of the dye is much bigger than the concentration of incoming Ca^{2+}, thus resulting in spectrum changes (see **Introduction**,

Figure 9) of only minor fraction of the dye molecules. The signal, gained by [fura-2-Ca^{2+}] complex, would have a large background coming from "non-activated" fura-2 molecules.
Secondly, a fraction of fura-2 molecules might not be able to chelate calcium ions at all, as a result of incomplete dye esterolysis (Yuste, 2000; Hougland, 1999). In fura-2 AM, all four carboxy-groups are esterified (**Figure 8**), thus enabling the dye to pass the cell membrane by passive diffusion. In the cell, incomplete esterolysis gives rise to mono-, di- and triacetomethoxy esters, fura-2 derivatives with strong fluorescence signal, which do not complex Ca^{2+} (*ibid.*). Both of these effects should be more pronounced as fura-2 concentration increases.

- *Analysis whether glutamate stimulation under our conditions induces excitotoxicity*

Excitotoxicity is glutamate-induced neuronal cell death, mediated by influx of calcium ions (Lee *et al.*, 1999; Miller *et al.*, 1998). Therefore, it shares the inducing agent with LTP/LTD, but activates different signal transduction pathways. For example, incubation in 500 µM glutamate inhibits calcium/calmodulin kinase II (CaMKII) activity in cultured hippocampal neurons, and causes "delayed cell death" (Churn *et al.*, 1995). One of the typical changes in neurons exposed to neurotoxic glutamate concentrations is accumulation of intracellular calcium (Burgard and Hablitz, 1995), *i.e.* failure of $[Ca^{2+}]_i$ to return to its basal level upon stimulus removal. We therefore tested whether 50 µM glutamate induced excitotoxicity in our system, although the concentrations reported to trigger glutamate-dependent cell death are higher (500 µM - Churn et al., 1995; 100 µM – Gray and Patel, 1995).
As demonstrated in Figures **22** and **23**, $[Ca^{2+}]_i$ returns to basal levels between the two stimuli, indicating that the influence of excitotoxicity in our experimental model can be neglected.

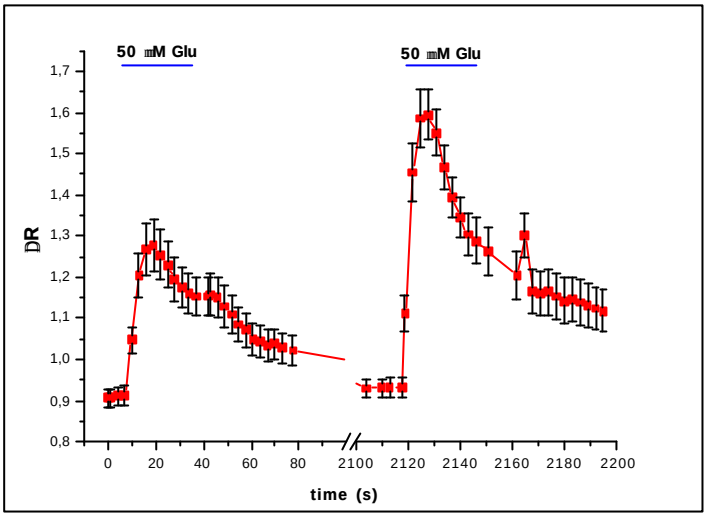

Figure 22. Calcium concentration returns to basal levels between the two stimulations. This suggests that during this time excitotoxicity has not been induced. Horizontal bars indicate duration of the 50 mM Glu stimuli (30 seconds). Trace represents the mean response of 33 cells. Error bars are s.e.m. Ratio images, from which the data for this graph were extracted, are shown in Figure 23.

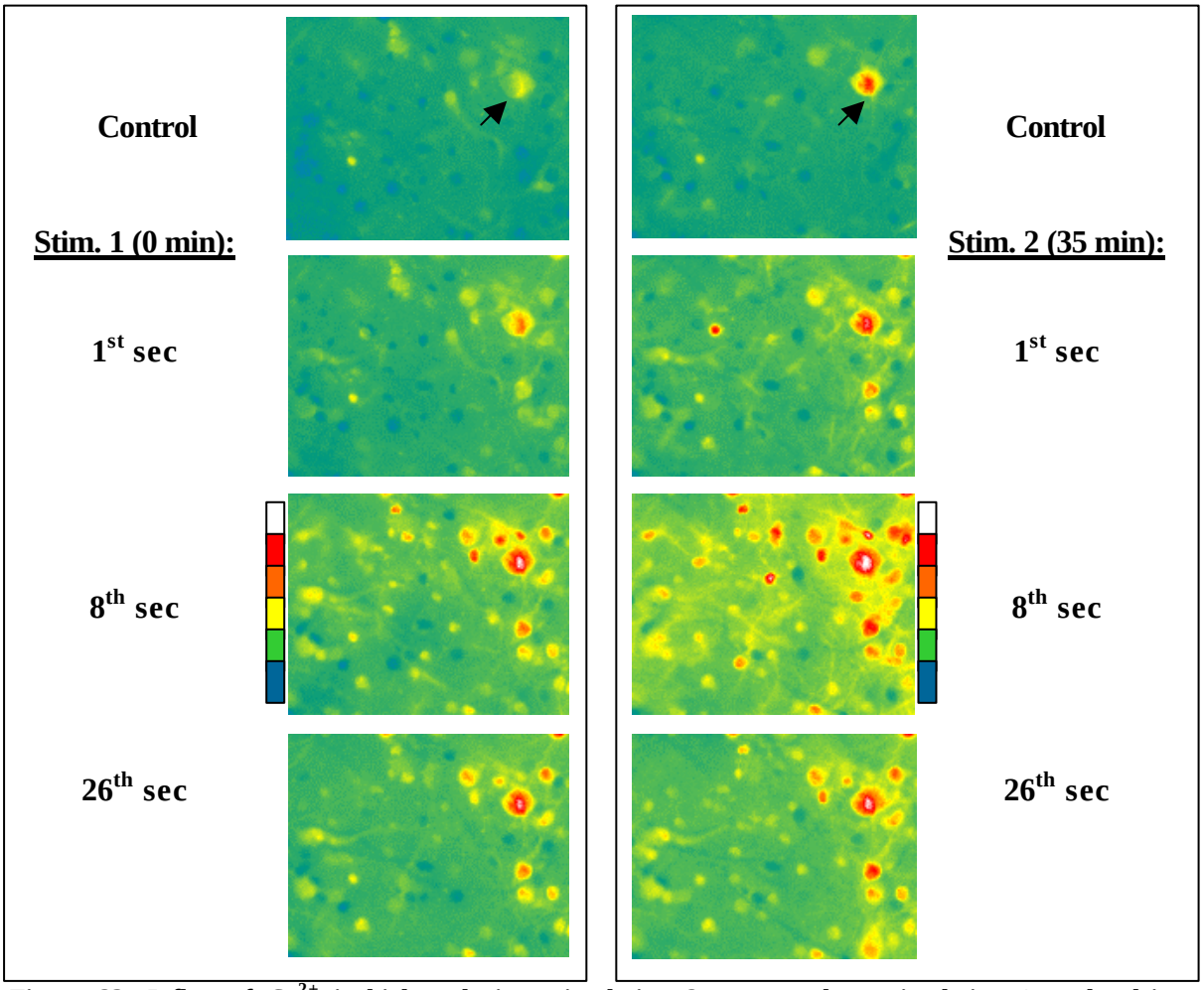

Figure 23. Influx of Ca^{2+} is higher during stimulation 2, compared to stimulation 1, and calcium concentration returns to its basal levels during the intermission (35 min). Colour intensity code: blue < green < yellow < red < white (blue: 0.60 white: 2.20 ratio units). This is a part of the ratio sequence that served as data source for the graph in Figure 22. Black arrows mark the cell that does not return to its basal state between the stimulations. Signals from such cells (usually 1- 2 per sample) were not used in the analysis.

- *Analysis of "contaminating" effects, due to the presence of glial cells*

There are two main classes of cells in the nervous system: nerve cells (neurons) and glial cells (glia) (Nicholls *et al.*, 1992). Central nervous system glia, as far as is known, are not directly involved in information processing, but they have other vital roles: physical support of neurons (Kandel *et al.*, 2000), growth factors release (Copelman *et al.*, 2000), scavenging toxic substances (Grewal *et al.*, 1997), neurotransmitter re-uptake (Porter and McCarthy, 1996), axon guidance (Hidalgo *et al.*, 1995), axon/dendrite insulation (Martini and Schachner, 1997) and forming blood-brain barrier (Vannucci *et al.*, 1997). Furthermore, there are between 10 and 50 times more glia than neurons in the central nervous system of vertebrates (Kandel *et al.*, 2000).

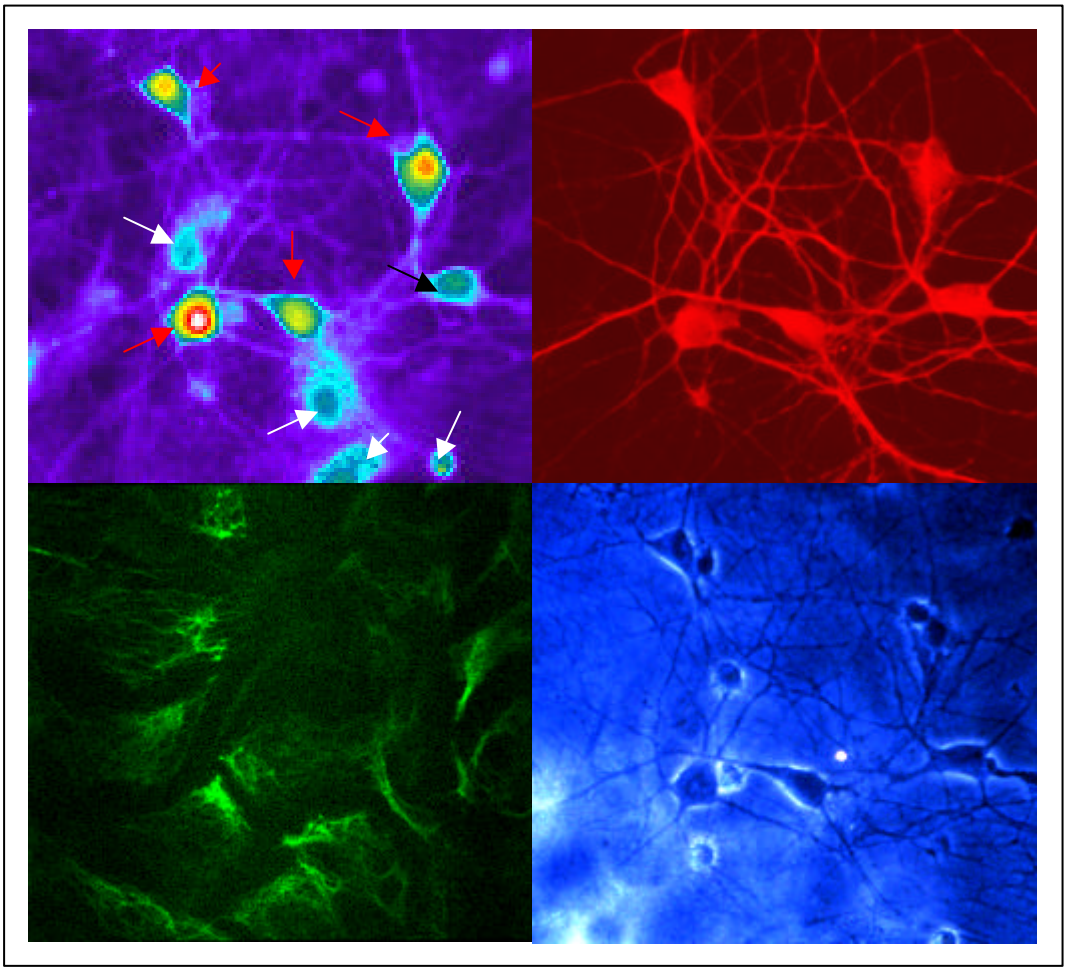

Figure 24. A group of fura-2 loaded cells from the glia-containing culture (DMEM/HS medium), indicating that the difference between neurons and glia could be told from the fluorescence images acquired under 340 nm illumination. Above, left: fura-2 loaded cells, illuminated by 340 nm light; Above, right: the same region, labelled with neuronal marker, anti-a-tau antibody; Beneath, left: the same region, labelled with glial marker, anti-GFAP antibody; Beneath, right: same region, seen under phase contrast. White arrows indicate the flat non-neuronal cells, which are not recognized by the neuron-specific antibody. Red arrows indicate neurons. Black arrow indicates one flat (dead?) neuron.

And although the glial cells are known to have modulatory effect on LTP/LTD (Wenzel *et al*., 1991) and possess functional glutamate receptors (Shelton and McCarthy, 1999), it has not been shown that their electrical responses could be potentiated as well. Our experiments were performed on neurons cultured in NeurobasalA/B27, a serum-free medium formulated by the research group of G.E. Brewer (Brewer *et al.*, 1993). NeurobasalA/B27 supports neuronal survival, whereas glial growth is reduced to 0.5% of the total, nearly pure neuronal population (*ibid.*).

Alternative to this approach is cell culturing in serum-containing media, typically 10% horse or foetal calf serum (Higgins and Banker, 1998). Under serum-containing conditions, however, glia grow and proliferate until a monolayer is formed. During this monolayer formation, neuronal growth is more and more suppressed, and the number of neurons decreases (*ibid.*). Glia growth can be inhibited by including anti-mitotic agents in the medium (*e.g.* cytosine-β-D-arabinofuranoside, *ibid.*). These agents, however, damage neuronal DNA as well (Park *et al.*, 1998).

Therefore, by choosing NeurobasalA/B27 medium for the cell culture, we minimized the possibility that the signals measured come from non-neuronal cell types. Additionally, we developed a method to differentiate between the neuronal and glial cells, based on cell body morphology/coloration. As seen in **Figure 24**, fluorescence images of fura-2-loaded cell bodies, illuminated by 340 nm light, could be divided into two groups: **1)** sharp, multicoloured, and **2)** diffuse-shaped, single-coloured ones. Immunostaining with neuronal and glial markers revealed that the first group could be identified as neurons (red arrows), whereas the second group (white arrows) are probably glial cell bodies.

Figure 25 illustrates where the difference in cell body coloration might come from. It is possibly a consequence of the hill-like form of the neuronal cell bodies, compared to flat cell bodies of the glial cells. Non-uniform neuronal cell height gives rise to a non-uniform amount of the dye (and, therefore, fluorescence intensity) excited by illumination, thus being represented by differently coloured areas (from blue-green to white). Glial cell bodies, on the contrary, have more uniform cell body height (*i.e.* do not vary much in amount of illuminated dye per optical path) and appear, therefore, mostly blue-green.

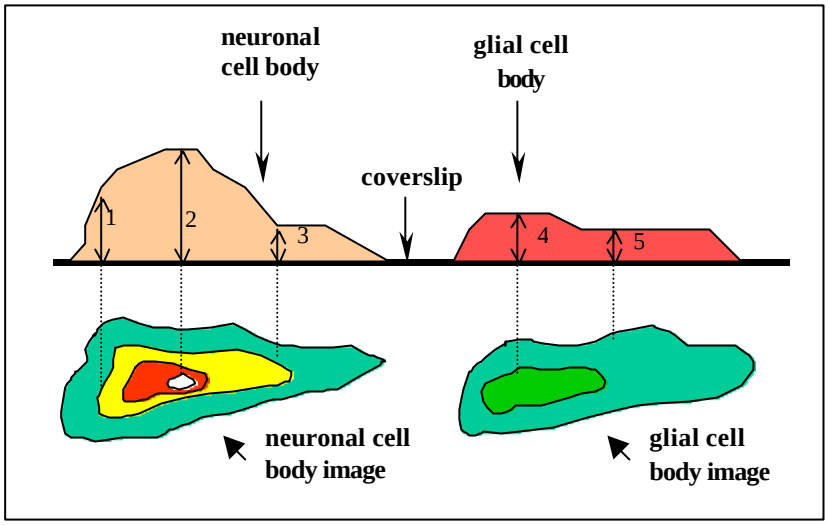

Figure 25. A possible explanation why fura-2-loaded neuronal and glial cell bodies appear differently coloured in 340 nm–illuminated fluorescence images. Different length of optical paths through the cell bodies (1, 2, 3: neuron; 4, 5: glial cell) determines different amounts of fura-2 molecules excited. This provides different coloration patterns of the two cell types, enabling their identification.

3.2 Pharmacological analogies of our system with electrophysiologically studied LTP

In the **Introduction**, an overview was given of the biochemical systems within neuronal cells, which give rise to LTP induction and maintenance. Robust increase of cytosolic calcium concentration in the postsynaptic cell is the first and most important event in the cascade (Revest and Longstaff, 1998). Since the glutamatergic system dominates hippocampal structures, there are several means of calcium entrance that could be opened, following presynaptic glutamate release. Firstly, there are ligand-gated Ca^{2+} channels, *e.g.* ion-channel glutamate receptors (NMDA, AMPA, kainate/quisqualate). They allow calcium ions from the intercellular space to enter dendritic spines, activating CaMKII-, PKC- and PKA-dependent signal transduction pathways (*ibid.*). Upon glutamate release, AMPA and kainate/quisqualate receptors get activated quickly, becoming permeable to Na^{+} and Ca^{2+} (Koh *et al.*, 1995). This cation influx induces depolarisation of the cell membrane, an event which relieves Mg^{2+} block of NMDA receptors, enabling calcium influx through glutamate-bound receptors (Ascher and Johnson, 1994). Secondly, such depolarization activates voltage-gated Ca^{2+} channels (VGCC) (Belhage *et al.*, 1996). Thirdly, stimulation of metabotropic glutamate receptors induces calcium outflow from intracellular stores, *i.e.* smooth endoplasmic reticulum (Bliss and Collingridge, 1993).

As eluded to in the **Introduction**, contribution of these (but not only these!) components is typical for LTP. In order to demonstrate that the enhancement of $[Ca^{2+}]_i$ induced by 50 μM glutamate in our system was LTP, we needed to demonstrate that the system in use depends on similar parameters. To achieve this, we performed a series of experiments where a 50 μM glutamate stimulus was applied to the cells, together with the appropriate antagonist for AMPA, NMDA and metabotropic glutamate receptors and a VGCC blocker. After 35 minutes, the stimulus was repeated and the difference in calcium ion influx (represented by the ratio values) was measured. Control condition in all experiments was the repeated 50 μM glutamate stimulus, which was able to induce Ca^{2+} influx potentiation in all the cases (as already depicted in **Figures 17** and **22**). To increase the probability that the particular receptor/channel type remains deactivated during the whole interval of stimulus duration, washing buffer containing an appropriate antagonist (or blocker, in the case of VGCC) was applied onto the cells prior to each stimulation, for 2 minutes.

- *Blocking of NMDARs with AP-5 prevents glutamate-induced potentiation*

The most extensively studied LTP type is the one of the hippocampal CA1 cells. It is usually induced electrically, either by tetanic or theta-pattern stimulation of Schaffer collaterals (Collingridge *et al.*, 1983). It is supposed to be of Hebbian nature, and it is NMDA receptor-dependent (*ibid.*). However, it should be mentioned again that in the hippocampus not all the cells express NMDAR-dependent LTP (Debray *et al.*, 1997). In order to investigate whether 50 μM glutamate-induced potentiation of Ca^{2+} influx that we observed in our system (**Figures 19** and **22**) was dependent on NMDA receptors, 25 μM of AP-5 (D-2-amino-5-phosphonopentanoic acid) was added to the 50 μM glutamate-containing stimulation buffer. (AP-5 is a widely used, competitive NMDAR antagonist: Jane *et al.*, 1994). Prior to each stimulation – as explained in the previous paragraph – cells were for 2 minutes incubated in washing buffer, containing 25 μM AP-5 as well. After first stimulation with glutamate/AP-5 mixture, cells were washed for 2 minutes and given the second glutamate/AP-5 stimulus after 35 minutes. The same procedure was repeated with the control groups of cells, except that they were treated with glutamate alone.

Under both conditions, the stimuli induced calcium ion influx. For each stimulus, ratio levels representing basal calcium concentration were subtracted from the ratio levels acquired immediately after application of the stimulation buffer ($\mathbf{DR = R_s - R_b}$: $\mathbf{R_s}$ – ratio during the stimulation; $\mathbf{R_b}$ – basal state ratio), resulting in the ratio increase for the given sti-

mulus (**DR**). Difference between the second and the first stimulus ($\mathbf{DR_T = DR_2 - DR_1}$) is the measure of Ca^{2+} influx potentiation ($\mathbf{DR_T} > 0$) or depotentiation ($\mathbf{DR_T} < 0$).

Figure 26 and **Table 9** summarize the results of such experiments. It can be seen that, under our conditions, the presence of AP-5 prevents glutamate-induced enhancement of calcium ion influx.

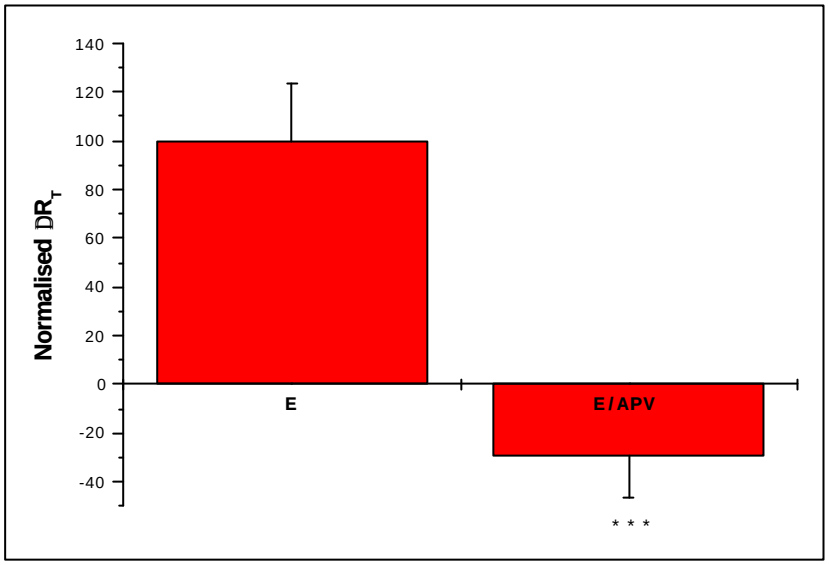

Figure 26. Competitive NMDAR antagonist AP-5 (E/APV) blocks the potentiating effect of 50 mM glutamate (E). Prior to each stimulation, cells from the E/APV group were incubated for 2 min in washing buffer containing 25 mM AP-5, and then stimulated for 30 s with 50mM Glu/25 mM AP-5. Following the washout of the stimulus (2 min), stimulation procedure was repeated (after 35 min). Control group of cells (E) was subjected to the same treatment, but without AP-5. For normalisation, mean potentiation (DR_T) induced in the control group was taken to be 100. Negative mean DR_T value in the E/APV group does not suggest that AP-5 induces depotentiation, since it does not differ significantly from 0 (one population t-test, 0.05 level: t = -1,673 ; p = 0,098). Percentage of de- and potentiated cells in E/APV group was 65.9 and 34.1, respectively. Control (E) group: 36.5 and 60.8. Number of experiments: 4. Error bars are s.e.m.

Two-population t-test at 0.05 level: t = -4.509 p = 1.266×10^{-5}
At the 0.05 level, the two means are significantly different.

Stimulus	Mean	s.d.	s.e.m.	Sum	N	Stat.sig.
E (control)	100	199.851	23.232	7400	74	-
E/APV	-29.296	161.484	17.515	-2490.188	85	***

Table 9. Coapplication of 25 mM AP-5, competitive NMDAR antagonist, prevents Ca^{2+} influx potentiation, induced by 50 mM glutamate. Prior to stimulation, cells were incubated for 2 min in washing buffer with 25 mM AP-5 and then stimulated for 30 s with 50mM Glu/25 mM AP-5. Following the washout of the stimulus (2 min), stimulation procedure was repeated (after 35 min). Control group of cells (E) was subjected to the same treatment, but without AP-5. Number of experiments: 4.

- *Blocking of AMPARs with CNQX does not prevent glutamate-induced potentiation*

Some forms of LTP are affected by non-NMDAR antagonists, including the LTP on CA3-CA1 synapses (Grover, 1998). In our system, blocking the AMPA receptors by 10 µM

CNQX (6-cyano-7-nitroquinoxaline-2,3-dione: a potent, competitive AMPA/kainate antagonist - Honoré *et al.*, 1988) produced diminished potentiation, but the mean ΔR_T value for CNQX-treated neurons did not differ significantly from the control group one (**Figure 27**, **Table 10**).

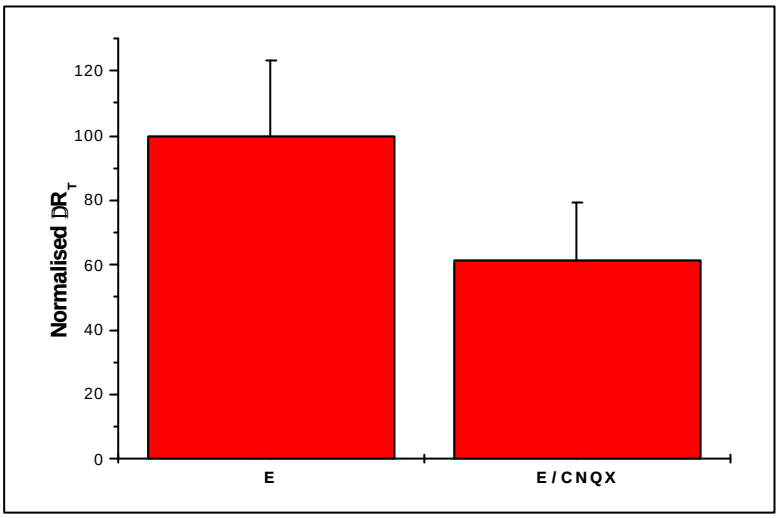

Figure 27. The AMPAR antagonist CNQX coapplication (E/CNQX) does not significantly affect 50 mM glutamate–induced potentiation (E). Prior to each stimulation, cells from the E/CNQX group were incubated for 2 min in washing buffer containing 10 mM CNQX, and then stimulated for 30 s with 50mM Glu/10 mM CNQX. Following the washout of the stimulus (2 min), stimulation procedure was repeated (after 35 min). Control group of cells (E) was subjected to the same treatment, but without CNQX. For normalisation, mean potentiation (ΔR_T) induced in the control group was taken to be 100. Percentage of de- and potentiated cells in E/CNQX group was 31.9 and 65.2, respectively. Control (E) group: 27.6 and 69. Number of experiments: 4. Error bars are s.e.m.

Two-population t-test at 0.05 level: t = -1.295 p = 0.197
At the 0.05 level, the two means are NOT significantly different.

Stimulus	Mean	s.d.	s.e.m.	Sum	N	Stat.sig.
E (control)	100	199.851	23.232	7400	74	-
E/CNQX	61.507	150.174	18.079	4243.966	69	-

Table 10. Coapplication of 10 mM CNQX, competitive AMPAR antagonist, does not affect significantly Ca^{2+} influx potentiation, induced by 50 mM glutamate. Prior to stimulation, cells were incubated for 2 min in washing buffer with 10 mM CNQX and then stimulated for 30 s with 50mM Glu/10 mM CNQX. Following the washout of the stimulus (2 min), stimulation procedure was repeated (after 35 min). Control group of cells (E) was subjected to the same treatment, but without CNQX. Number of experiments: 4.

- *Blocking of mGluRs with MCPG prevents glutamate-induced potentiation*

Activation of metabotropic glutamate receptors is required for induction of long-term potentiation in the hippocampus, as shown in the studies with mGluR antagonists (Bortolotto *et al.*, 1994; Bortolotto and Collingridge, 1999). Therefore, to examine the influence of glutamate-induced potentiation in our system, we performed experiments where 500 µM MCPG ((S)-α-methyl-carboxyphenylglycine: non-selective mGluR I/II antagonist - Watkins

and Collingridge, 1994) was coapplied with 50 µM glutamate. Data obtained from such experiments are summarized in **Figure 28** and **Table 11**, suggesting that the cells, treated with the mGluR antagonist, do not show enhancement in Ca^{2+} influx as a result of glutamate stimulation.

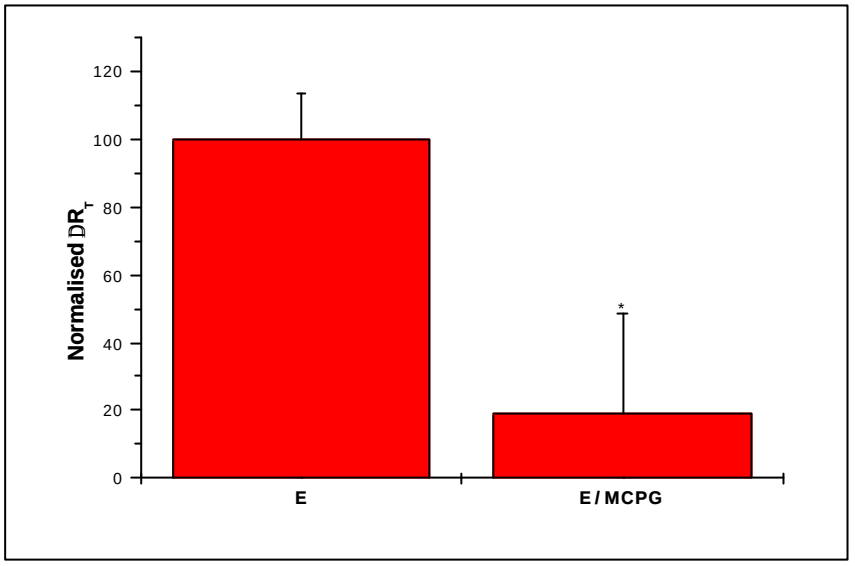

Figure 28. Non-selective mGluR antagonist MCPG (E/MCPG) blocks the potentiating effect of 50 mM glutamate (E). Prior to each stimulation, cells from the E/MCPG group were incubated for 2 min in washing buffer containing 500 mM AP-5, and then stimulated for 30 s with 50mM Glu/500 mM MCPG. Following the washout of the stimulus (2 min), stimulation procedure was repeated (after 35 min). Control group of cells (E) was subjected to the same treatment, but without MCPG. For normalisation, mean potentiation (DR_T) induced in the control group (E) was taken to be 100. Positive mean DR_T value in the E/MCPG group does not suggest that glutamate/MCPG coapplication induces (small) potentiation, since it does not differ significantly from 0 (one population t-test, 0.05 level: t = 0,627 ; p = 0,534). Percentage of de- and potentiated cells in E/MCPG group was 60.5 and 37.2, respectively. Control (E) group: 15.6 and 77.2. Number of experiments: 3. Error bars are s.e.m.

Two-population t-test at 0.05 level: t = -2.787 p = 0.006
At the 0.05 level, the two means are significantly different.

Stimulus	Mean	s.d.	s.e.m.	Sum	N	Stat.sig.
E (control)	100	108.128	13.310	6599.963	66	-
E/MCPG	18.725	195.760	29.853	805.168	43	*

Table 11. Coapplication of 500 mM MCPG, non-specific mGluR antagonist, prevents Ca^{2+} influx potentiation, induced by 50 mM glutamate. Prior to stimulation, cells were incubated for 2 min in washing buffer with 500 mM MCPG and then stimulated for 30 s with 50mM Glu/500 mM MCPG. Following the washout of the stimulus (2 min), stimulation procedure was repeated (after 35 min). Control group of cells (E) was subjected to the same treatment, but without AP-5. Number of experiments: 3.

- Blocking of VGCCs with nifedipine does not prevent glutamate-induced potentiation

Voltage-gated calcium channels (especially L-type) play a significant role in tetanus- and tetraethylammonium chloride (TEA)-induced LTP (Grover, 1998; Huber *et al.*, 1995). To test whether these ion channels influence glutamate-induced Ca^{2+} potentiation in our sys-

tem, we included 10 µM nifedipine (1,4-dihydro-2,6-dimethyl-4-(2-nitrophenyl)-3,5-pyridinedicarboxylic acid dimethyl ester: L-type VGCC blocker - Tomlinson *et al.*, 1993) in our stimulation buffer. Comparison between the changes induced by glutamate and glutamate/nifedipine coapplication are depicted in **Figure 29** and **Table 12**. Non-significantly weaker decrease in Ca^{2+} influx potentiation was observed.

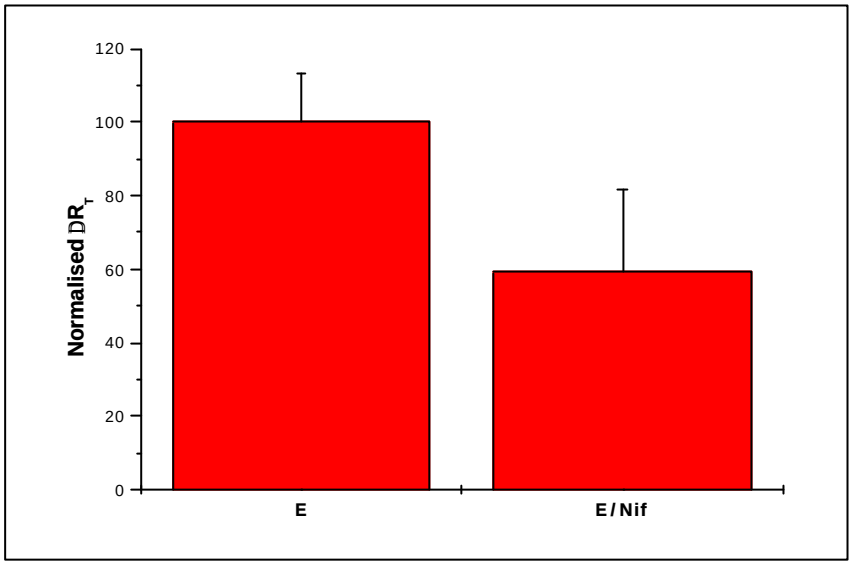

Figure 29. The VGCC blocker nifedipine coapplication (E/Nif) does not significantly affect 50 mM glutamate–induced potentiation (E). Prior to each stimulation, cells from the E/Nif group were incubated for 2 min in washing buffer containing 10 mM nifedipine, and then stimulated for 30 s with 50mM Glu/10 mM nifedipine. Following the washout of the stimulus (2 min), stimulation procedure was repeated (after 35 min). Control group of cells (E) was subjected to the same treatment, but without nifedipine. For normalisation, mean potentiation (ΔR_T) induced in the control group was taken to be 100. Percentage of de- and potentiated cells in E/Nif group was 21.9 and 73.2, respectively. Control (E) group: 13.6 and 81.9. Number of experiments: 3. Error bars are s.e.m.

Two-population t-test at 0.05 level: t = -1.660 p = 0.099
At the 0.05 level, the two means are NOT significantly different.

Stimulus	Mean	s.d.	s.e.m.	Sum	N	Stat.sig.
E (control)	100	108.127	13.310	6599.963	66	-
E/Nif	59.503	143.176	22.360	2439.635	41	-

Table 12. Coapplication of 10 mM nifedipine, L-type VGCC blocker, does not affect significantly Ca^{2+} influx potentiation, induced by 50 mM glutamate. Prior to stimulation, cells were incubated for 2 min in washing buffer with 10 mM nifedipine and then stimulated for 30 s with 50mM Glu/10 mM nifedipine. Following the washout of the stimulus (2 min), stimulation procedure was repeated (after 35 min). Control group of cells (E) was subjected to the same treatment, but without nifedipine. Number of experiments: 3.

3.3 Modulation of glutamate-induced potentiation by nicotine and galanthamine

In the **Introduction,** there is a short description of Alzheimer's disease (AD) symptoms and a treatment strategy (Alberca *et al.*, 2000; Schrattenholz *et al.*, 1996). It has been

mentioned that the approved AD medication modulates nicotinic currents by temporarily blocking AChE activity and, in the case of galanthamine, also by allosterical modulation of nicotinic acetylcholine receptors (Schrattenholz *et al.*, 1996). Nicotinic receptors have been shown to modulate long term potentiation (Fujii *et al.*, 1999; Fujii *et al.*, 2000). Since they belong to the family of ion channel receptors and allow Na^+ and Ca^{2+} influx, it was interesting to see whether and how nicotine application and co-application with glutamate increase intracellular calcium concentration. Applying nicotine on primary hippocampal cells in the range of 1 to 500 µM gave no rise to any changes in fura-2 fluorescence (data not shown). However, if coapplied with 50 µM glutamate at the concentration of 100 µM, nicotine seems to influence glutamate-induced Ca^{2+} influx potentiation. Two populations of neurons were clearly seen: the one that augments glutamate-induced potentiation effect, and the one that reverses it (**Figure 29, Table 13**).

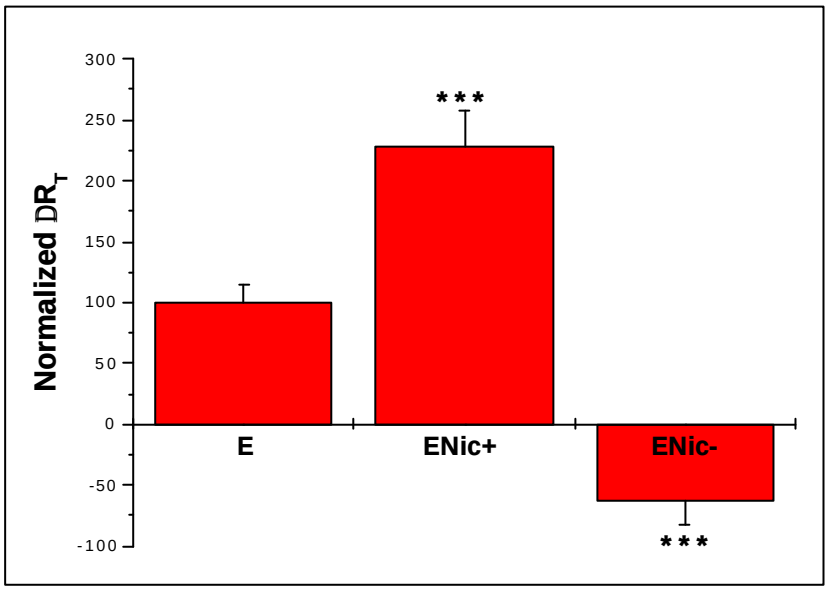

Figure 29. Nicotine co-application (at 100 mM) can either augment (ENic+) or diminish (ENic-) glutamate-induced potentiation (E). Nicotine (100 mM) has been co-applied with 50 mM glutamate for 30 sec, inducing ratio increase DR_1. Thirty-five minutes after washout, the stimulus was repeated, inducing ratio increase DR_2. Control group of cells (E) was subjected to the same treatment, but without nicotine. For normalisation, mean potentiation ($DR_T = DR_2 - DR_1$) induced in the control group (E) was taken to be 100. Percentage of de- and potentiated cells in E, ENic+ and ENic- groups were 16 and 84, 8.6 and 91.4, 65.2 and 34.8, respectively. Number of experiments: 3. Error bars are standard error of mean.

Two-population t-test at 0.05 level:
E *vs*. ENic+: t = 4.045, p = 8.305 x 10^{-5}; E *vs*. ENic-: t = -6.596, p = 4,455 x 10^{-10}
At the 0.05 level, the two means are significantly different.

Stimulus	Mean	s.d.	s.e.m.	Sum	N	Stat.sig.
E	100	161.396	14.858	11799.957	118	-
ENic+	227.887	173.679	29.357	7976.036	35	***
ENic-	-63.351	160.636	19.773	-4181.103	66	***

Table 13. Nicotine co-application (at 100 mM) can either augment (ENic+) or diminish (ENic-) glutamate-induced potentiation (E). Nicotine (100 mM) has been coapplied with 50 mM glutamate for 30 sec. Thirty-five minutes after washout, stimulus was repeated. Control group of cells (E) was subjected to the same treatment, but without nicotine and nicotine/galanthamine coapplication. For normalisation, mean potentiation ($DR_T = DR_2 - DR_1$) induced in the control group was taken to be 100. Percentage of de- and potentiated cells in E, ENic and ENicGal groups were 16 and 84, 8.6 and 91.4, 65.2 and 34.8, respectively. Number of experiments: 3. Error bars are standard error of mean.

Whichever effects nicotine might exert on glutamate-induced potentiation, they remain unchanged when galanthamine (0.5 µM) is added to stimulation mixture (data shown for "negative" nicotine population, **Figure 30, Table 14**).

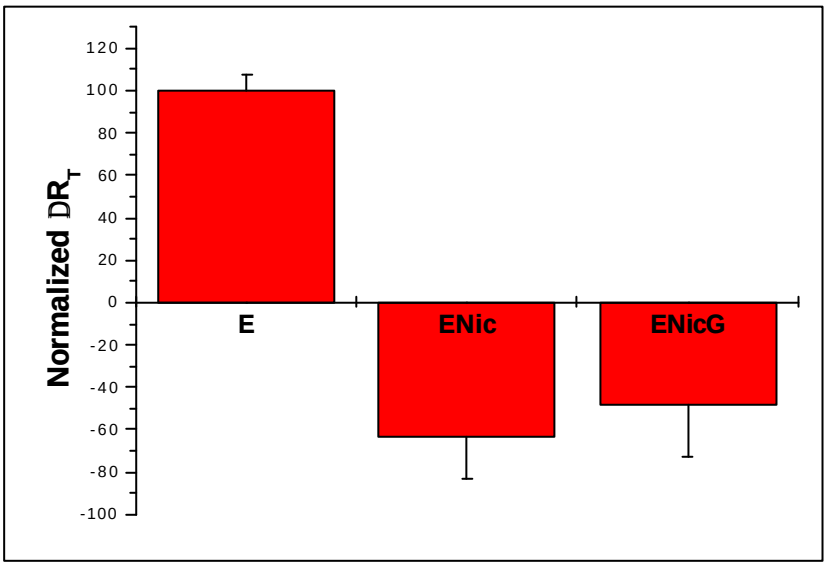

Figure 30. Galanthamine (ENicG) coapplication does not influence nicotine modulation (ENic) of glutamate-induced potentiation (E). Nicotine (ENic: 100 mM) and nicotine/galanthamine mixture (ENicG: 100/0.5 mM) have been coapplied with 50 mM glutamate for 30 sec, inducing ratio increase DR_1. Thirty-five minutes after washout, stimulus was repeated, inducing ratio increase DR_2. For normalisation, mean potentiation ($DR_T = DR_2 - DR_1$) induced in the control group (E) was taken to be 100. Percentage of de- and potentiated cells in E, ENic and ENicGal groups were 9.6 and 87.5, 66.7 and 33.3, 60 and 36, respectively. Number of experiments: 3. Error bars are standard error of mean.

Two-population t-test at 0.05 level:
ENic *vs*. ENic/Gal: t = 0.418 p = 0.677
At the 0.05 level, the two means are NOT significantly different.

Stimulus	Mean	s.d.	s.e.m.	Sum	N	Stat.sig.
E	100	90.903	7.794	13599.862	136	-
ENic	-63.350	160.635	19.772	-4181.102	66	-
ENicG	-48.572	119.412	23.882	-1214.302	25	-

Table 14. Galanthamine (ENicG) coapplication does not influence nicotine modulation (ENic) of glutamate-induced potentiation (E). Nicotine (100 mM) and nicotine/galanthamine mixture (100/500 mM) have been co-applied with 50 mM glutamate for 30 sec. Thirty-five minutes after washout, stimulus was repeated. (E – control (glutamate only); ENic – glutamate/nicotine coapplication; ENicG – glutamate/nicotine/galanthamine coapplication) Number of experiments: 3.

However, if glutamate is coapplied with galanthamine alone, control potentiation increases significantly. Interpretation of this effect as a consequence of AChE blockage is not supported by the fact that another anti-cholinesterase, rivastigmine (0.5 μM), coapplied with glutamate, contributes to values closer to the control ones (**Figure 31, Table 15**). Significance of this observation is supported by the two-population t-test at the 0.05 level. However, another statistical procedure, Kruskal-Wallis Statistics, does not confirm this (KW = 3.314 (corrected for ties) The P value is 0.1907, considered NOT significant)[1].

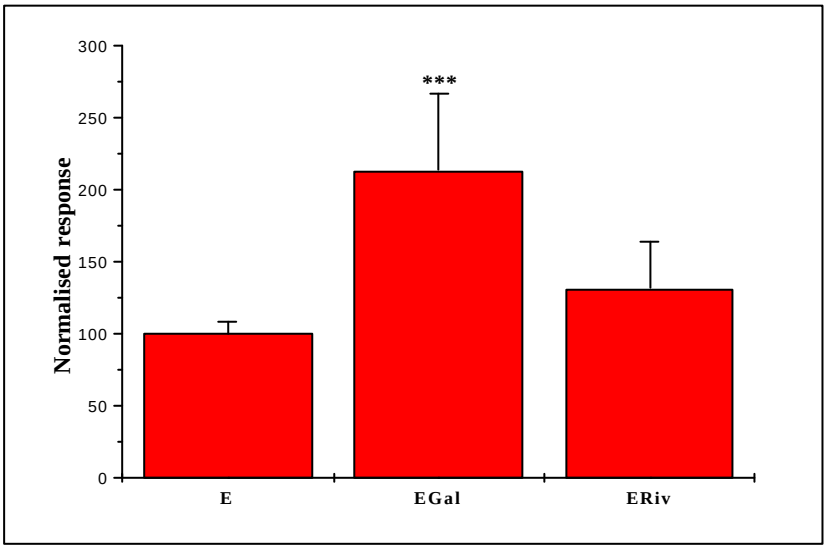

Figure 31. Galanthamine coapplication (EGal) can increase glutamate-induced potentiation (E). Augmentation induced by rivastigmine co-application (ERiv) is not statistically significant, therefore suggesting that the galanthamine-induced increasment in potentiation is not the consequence of AChE inhibition. Galanthamine (0.5 mM) and rivastigmine (0.5 mM) have been coapplied with 50 mM glutamate for 30 sec inducing ratio increase DR_1. Thirty-five minutes after washout, stimulus was repeated, inducing ratio increase DR_2. For normalisation, mean potentiation ($DR_T = DR_2 - DR_1$) induced in the control group (E) was taken to be 100. Percentage of de- and potentiated cells in E, EGal and ERiv groups were 9.6 and 89.0, 0 and 100, 10 and 82.5, respectively. Number of experiments: 2.

[1] KW analysis belongs to the group of non-parametric tests, which do not suppose that the values follow Gaussian distribution. It is therefore more strict than t-test or ANOVA.

Two-population t-test at 0.05 level:
E *vs*. EGal: t = 3.517 p = 5.573 x 10^{-4}
At the 0.05 level, the two means are significantly different.
E *vs*. ERiv: t = 1.385 p = 0.168
At the 0.05 level, the two means are significantly different.

Stimulus	Mean	s.d.	s.e.m.	Sum	N	Stat.
E	100	90.903	7.794	13599.862	136	-
EGal	213.188	338.014	53.444	8527.536	40	***
ERiv	131.159	202.873	32.077	5246.376	40	-

Table 15. Influence of anti-cholinesterases on glutamate-induced potentiation. Galanthamine (0.5 mM) and rivastigmine (0.5 mM) were co-applied with 50 mM glutamate for 30 sec. Thirty-five minutes after washout, stimulus was repeated. (E – control (glutamate only); EGal – glutamate/galanthamine coapplication; ERiv – glutamate/rivastigmine coapplication) Number of experiments: 2.

Incoherence between these two statistical interpretations arises from the big dispersion of EGal values, and probably means that the possible effect is best to be addressed individually, from cell to cell (**Figure 32**).

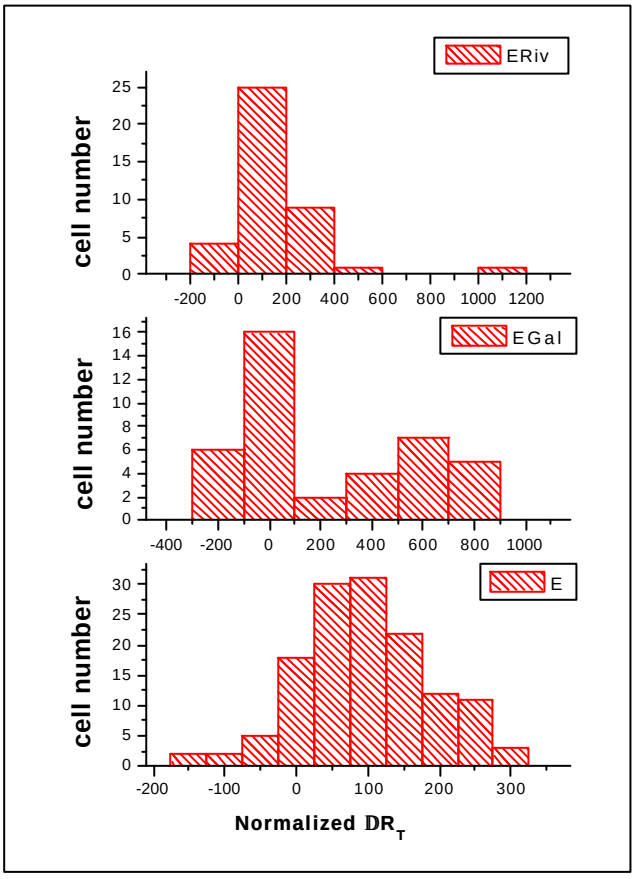

Figure 32. Distribution of Ca^{2+} influx potentiation (DR_T) among the cells, induced by glutamate (E), glutamate/galanthamine (EGal) and glutamate/rivastigmine (ERiv) application. Galanthamine (0.5 mM) and rivastigmine (0.5 mM) have been coapplied with 50 mM glutamate for 30 sec. Thirty-five minutes after washout, stimulus was repeated. See also Figure 31. Number of experiments: 2.

4. DISCUSSION

4.1 Selection of the method applied for LTP measurement

It has been mentioned (**Introduction**, p. 12) that calcium imaging has not played a dominant role as a tools for research on neuronal plasticity phenomena. A key reason for this is probably the type of information that can be extracted from the experimental system. Long-term potentiation (LTP) and long-term depression (LTD) are primarily (defined as) *electrical* features, and variables that could affect them are most precisely measured by means of electrophysiology. Moreover, such experiments are well suited for studies on slice preparations.

Calcium imaging measurements could not have been employed before the appropriate fluorescence dyes (in the early 80's) came into use (Haugland, 1999). Nowadays, a multitude of dyes is available, ranging from UV- to visible light-excitable, covering wide range of dissociation constants for calcium binding (approx. 50 nM – 50 μM, see Haugland, 1999; Tsien and Pozzan, 1989; Kao, 1994; Scheenen *et al*, 1998; Silver, 1998). In spite of the fact that "rule of the thumb" criteria regarding choice of the probe, its loading protocol and way of measurement exist, it should be pointed out that fine tuning of such variables is remarkably system-sensitive. In the initial phase of this work two calcium-binding dyes have been tested, fura-2 and fluo-3. Since the signals obtained from cells incubated in fura-2 AM and fluo-3 AM were of similar intensity, we decided to use the former, due to its suitability to ratiometric measurements. (Fluo-3 measurements are performed using single excitatory wavelength, thus giving rise to results which are distorted by bleaching (Haugland, 1999).) Two cell culture media – serum-containing and serum-free - were also tried. The former provides cultures populated by neurons and glia (**Results, Figure 24;** Higgins and Banker, 1998), whereas the latter supports almost exclusively neuronal growth (Brewer *et al.*, 1993). More reproducible signals were recorded from the serum-free system, and it was therefore used in all LTP experiments. Culturing and imaging of organotypic hippocampal slices (Gähwiler *et al.*, 1998) was also tried, but success of each preparation was very prone to variations and, therefore, unsuitable.

Other research groups used fluorescent measurement of calcium ion levels in LTP/LTD research only as an accessory tools, usually to elucidate calcium dynamics in dendritic spines, whereas the actual measurement of potentiation/depotentiation was performed electrophysiologically. These studies covered "normal" and laser scanning microscopy and utilised various calcium-sensitive dyes: **quin2** (Minota *et al.*, 1991; Williams and Johnston, 1989), **fura-2** (Hansel *et al*., 1997; Wu and Saggau, 1994; Abe and Saito, 1992; Tekkök *et al.*,

1999; Isomura and Kato, 1999; Zheng *et al.*, 1996; Larkum *et al.*, 1994; Regher and Tank, 1991), **rhod-2** (Yasuda and Tsumoto, 1996) and **fluo-3** (Tekkök *et al*, 1999).

4.2 Description of the system used for biochemical studies of LTP

- *An appropriate glutamate concentration for LTP induction*

A necessary prerequisite for this work was to determine a glutamate concentration at which a) calcium influx is predominately up-regulated (as detected by repeated application), and b) would not trigger excitotoxicity, another important effect related to glutamate exposure[1]. Since a key step in LTP formation is a large rise in intracellular concentration of calcium ions, it was inevitable to find a glutamate concentration which was sufficiently high to induce potentiation, but too low to induce excitotoxicity.

Based on the glutamate dose-response curves (see **Results**, **Figures 14, 16**), we used a 50 μM Glu stimulus. This concentration provides a calcium influx of high intensity, localized at the upper plateau of the sigmoidal, dose-response curve. If the dose-response curve is obtained from the recordings performed by applying increasing glutamate concentrations to the one group of cells (**Figure 14**, EC_{50} = 5.6 ± 0.3 μM), glutamate concentrations above 10 μM appear to elicit maximal response. However, in the case of dose-response curve where the responses for each concentration were recorded from the previously non-stimulated cell group (**Figure 15**, EC_{50} = 18 ± 5 μM), the smallest stimulus that elicits upper plateau response appears to be about 50 μM. Additionally, if the absolute response to 50 μM glutamate, taken from the "pre-stimulation" dose-response curve (**Figure 14**) is compared to the 50 μM glutamate response of naïve, previously glutamateuntreated cells, it can be seen that the mean ratio increase is 2.19 times larger in the latter case (**Figure 16, Table 2**). This suggests that previous stimuli affect later responses, and that the smallest glutamate concentration to induce plateau response is rather 50 μM than 10 μM. Another argument for using 50 μM glutamate stimulus (application time 30 s) for LTP induction is its ability to potentiate Ca^{2+} influx stronger than the 100 μM one (**Figure 19**).

[1] Excitotoxicity, a glutamate-induced neuronal cell death, is triggered by high intracellular calcium levels and depends on NMDA- and AMPA-receptors. For excellent and up-to-date coverage on this subject, see Lee *et al*., 1999; also Miller *et al*., 1998.

The same stimulus (50 μM glutamate, 30s) for LTP induction was used by Malgaroli and Tsien in 1992. The model system in their study was primary culture of hippocampal neurons as well, but the potentiation was measured electrophysiologically. These authors reported 70% of potentiated cells, whereas in our experiments their number varied from 60.8% to 100%. Zilberter *et al*. (1990) induced short-lasting (about 10 min) enhancement of responsiveness in acutely isolated hippocampal cells, by employing a perfusion device which delivered stimulating solution (400 μM glutamate, 5 μM glycine) at 20 Hz. Chemical induction has also been used to induce LTP (Izumi et al., 1987; Cormier et al., 1993; Musleh et al., 1997) in hippocampal slices. In all of these cases, chemically triggered LTP shared major properties with its electrically induced counterpart: it was NMDAR- and mGluR-dependent. Additionally, chemically induced LTP could not be further potentiated by electrical stimuli, suggesting that the two stimulation protocols may activate same biochemical machinery.

Study	System	Stimulus type	Duration	Property	Detection
Izumi *et al*. '87	Acute slice	100 μM Glu, 15 mM K^+	5 min	LTP	Electrical
Ziberter *et al*. '90	Isolated cells	400 μM Glu, 5 μM Gly	20 Hz, 15 s	STP	Electrical
Malgaroli, Tsien '92	Cell culture	50 μM Glu	30 s	LTP	Electrical
Cormier *et al*. '93	Acute slice	1 M Glu	5 pulses, 10 s	LTP	Electrical
Musleh *et al*. '97	Slice culture	10 mM Gly	"brief"	LTP	Electrical

Table 20. An overview of studies where potentiation was chemically induced. Every experimental system was of hippocampal origin. STP is short-term potentiation. In all of the cases, detection was electrical.

- *Analysis of fura-2 AM concentration effects on the glutamate-induced potentiation*

As shown in **Figure 20,** 50 μM glutamate-induced potentiation is significantly stronger if the cells were incubated in 2 μM fura-2 AM solution, compared to 20 μM fura-2 AM-incubated cells. Furthermore, under the two incubating conditions, mean calcium ion influx upon the first glutamate stimulus appears to be nearly five times larger in the group of cells incubated in 2 μM fura-2 AM (**Figure 21**).

Loading protocol by passive diffusion is based on cell incubation in a solution containing acetomethoxy- (AM) esters of the dye (Takahashi *et al.*, 1999). Such esters are hydrophobic enough to pass the cell membrane. Upon cell entrance, ester bonds (four in the case of fura-2 AM: Yuste, 2000; Hougland, 1999) are cleaved by intracellular esterases, yielding the dye molecule with four free carboxy-groups, which can chelate calcium ions. Furthermore, the dye molecules after esterolysis can not exit the cell passively, due to increased polarity (*ibid.*).

A consequence of this is unchanged gradient of fura-2 AM concentration in the solution (always smaller [fura-2 AM] in intracellular space, compared to the extracellular), giving rise to dye upconcentration within the cells (i.e. $[\text{fura-2}]_i > > [\text{fura-2 AM}]_e$). It has been demonstrated that the final hydrolysed concentration of calcium-chelating dye quin-2 can be several hundred times that of the initial concentration of the ester in the loading solution (Tsien *at al.*, 1982). Therefore, the difference in intensity and potentiation of Ca^{2+} influx between the cell groups incubated in different fura-2 AM-containing solutions (**Figures 20** and **21**) might arise from (a) much larger concentration in intracellular fura-2 (>> 20 μM in the cells incubated in 20 μM fura-2 AM solution) and (b) incomplete dye hydrolysis (Takahashi *et al.*, 1999), which should also be more pronounced with the increased dye concentration. In the former case, dye concentration in the cells incubated in 20 μM fura-2 AM would be significantly larger than the concentration of intracellular Ca^{2+} during the stimulation (it is generally accepted that the $[Ca^{2+}]_i$ does not exceed 5 μM: Bear *et al.*, 1995). Therefore, the more dye is used for loading, the bigger is the background coming form the dye molecules not bound to calcium ions. Effects coming form the latter case (incomplete dye hydrolysis) would be similar: background fluorescence would be produced by the dye molecules unable to chelate Ca^{2+}.

The optimal dye loading concentration should therefore be high enough to provide sufficiently strong signal, but also low enough, in order not to induce large background. In our system, it was 2 μM (cells incubated in 1 μM fura-2 AM gave rise to very weak signals).

- *Analysis whether glutamate stimulation under our conditions induces excitotoxicity*

Figures 22 and **23** illustrate that intracellular $[Ca^{2+}]$ returns to its basal level between the two stimulations by 50 μM glutamate. As mentioned in the **Results**, this suggests that the glutamate stimulus did not activated the signal transduction pathway which leads to neuronal death. Burgar and Hablitz (1995) have shown that the exposure of neurons to excitotoxicity-inducing glutamate concentrations correlates with failure of $[Ca^{2+}]_i$ to return to its basal level upon stimulus removal. Glutamate concentrations reported to trigger "delayed cell death" cover the range from 100 (Gray and Patel, 1995) to 500 μM (Churn *et al.*, 1995).

4.3 Pharmacological analogies of our system with electrophysiologically studied LTP

Based on a suggestion by Fazeli and Collingridge (1996), LTP can be classified according to: a) the component (receptor) which is required for LTP induction, and b) the component (receptor) whose response is actually potentiated. Therefore, we can talk about an LTP dependent on (triggered by) component A, and mediated by component B. Combinations of AMPAR-mediated (both NMDA-dependent and –independent) and NMDAR-mediated (NMDAR- and mGluR-dependent) LTP are most frequently encountered (*ibid.*). This classification can only partly be useful in evaluation of the results presented in this work, since our experimental design excluded investigation of A-dependent/A-mediated events. As an illustration, it was impossible to investigate NMDAR-dependent/NMDAR-mediated LTP, since, in our experiment aimed at determining NMDAR influence on LTP, both stimuli contained AP-5, an NMDAR antagonist. However, such a scheme still allows for NMDA-dependent/AMPA-mediated and mGluR-dependent/AMPA/NMDA-mediated LTPs.

- *Blocking of NMDARs with AP-5 prevents glutamate-induced potentiation*

As summarised in **Figure 26** and **Table 9**, 50 μM glutamate-induced potentiation of Ca^{2+} influx could be prevented, if 10 μM AP-5 (D(-)-2-amino-5-phosphonopentanoic acid: a widely used, competitive NMDAR antagonist: Jane *et al*., 1994) was included in the stimulation buffer. Both *in vitro* (Collingridge et al. in $1983_{a,b}$; Harris *et al.*, 1984) and *in vivo* (Morris *et al.*, 1986) studies have demonstrated the ability of AP-5 to prevent LTP induction. However, not all the cells in our study exerted the same behavior – in the presence of AP-5 there was still 34.1% of potentiated cells (**Figure 26**). This may be supported by observations that, in addition to NMDAR-dependent LTP (found to occur in CA1, lateral and medial perforant pathways, dentate gyrus granule cells and the commissural-associational pathway to CA3: Colino and Malenka, 1993; Errington *et al.*, 1987; Morris *et al.*, 1986), there are hippocampal cells which comprise to NMDAR-independent LTP, *i.e.* the ones from the CA3 region (Alger and Teyler, 1976; Zalutsky and Nicoll, 1990). Since our cell cultures were prepared by dissociating whole hippocampi, it must be taken into account that a fraction of the cells observed did not come from regions where the NMDAR-dependent LTP was localized. Quantitative estimations regarding the number of particular cell types in rat hippocampus (1,000,000 granule cells, 250,000 belonging to CA1 and 160,000 to CA3: Shepherd, 1998) are an argument that further strengthens this explanation.

- *Blocking of AMPARs with CNQX does not prevent glutamate-induced potentiation*

In our experimental system, groups of cells stimulated by 50 μM glutamate and 50 μM Glu/10 μM CNQX (6-cyano-7-nitroquinoxaline-2,3-dione: a potent, competitive AMPA/kainate antagonist - Honoré *et al*., 1988) showed no statistically significant difference in calcium influx potentiation (**Figure 27, Table 10**). Fraction of potentiated cells was also similar (69% by glutamate; 65.2% by glutamate/CNQX). Experiments of Kauer *et al*. (1988) performed on CA1 synapses demonstrated that, following blockade of AMPAR with CNQX, high frequency stimulation induced a full amplitude LTP. Those data comprised to the most accepted model for LTP induction (**Introduction, Figure 5**: fast transmission mediated by AMPAR Na^+ entry membrane depolarisation relieving Mg^{2+} block from NMDAR NMDAR activation cal cium influx LTP induction), which assumes that the AMPARs can be by-passed, without disabling the long term potentiation. However, using the same model system (CA1 synapses), Debray and colleagues (1997) have shown that AMPA blockade with CNQX disables the induction of NMDA-dependent LTP, but also leads to the voltage-gated calcium channel (VGCC)-dependent one, blocked by nifedipine (*vide infra*).

- *Blocking of mGluRs with MCPG prevents glutamate-induced potentiation*

Our data (**Figure 28, Table 11)** indicate that 50 μM glutamate stimulus fails to induce potentiation of calcium ion influx if the metabotropic glutamate receptors were blocked by MCPG ((S)-α-methyl-carboxyphenylglycine), a non-selective mGluR I/II antagonist (Watkins and Collingridge, 1994). Contribution of potentiated and depotentiated cells was 37.2% and 60.5%, respectively, being similar with values obtained by blockade of NMDARs by AP-5 (**Figure 26, Table 9**). In electrophysiological studies, MCPG was shown to reversibly block LTP in CA1, thus demonstrating the absolute requirement for the mGluR activation by synaptically released glutamate in the LTP induction (Bashir *et al.*, 1993). In 1994, Bortolotto *et al.* blocked with MCPG the LTP induction at non-conditioned synapses, *i.e.* at those where no activation of the mGluR had occurred previously. Importance of mGluRs for LTP induction was further emphasised by the experiments performed with ACPD (amino-cyclopentane-1S,3R-dicarboxylate), a group I/II mGluR agonist (Knöpfel *et al.*, 1995). In presence of this agonist, short-term potentiation and LTP of the field EPSP in CA1 region were greatly enhanced, compared with control slices (McGuinness *et al.*, 1991). This was confirmed in later stu-

dies by Behnisch and Reymann (1992). Moreover, tetanically induced short-term potentiation lasting 30 min was converted into LTP in the presence of 25 μM *trans*-ACPD (Aniksztejn *et al.*, 1992). ACPD can also induce a much faster onset LTP (peak attained in less than 10 min), providing that NMDAR and mGluR are activated coincidently. Thus, in the dentate gyrus, application of ACPD combined with membrane depolarization sufficient to induce NMDAR activation rapidly let to the induction of LTP (Connor *et al.*, 1995).

- Blocking of VGCCs with nifedipine does not prevent glutamate-induced potentiation

If a L-type VGCC blocker, nifedipine (1,4-dihydro-2,6-dimethyl-4-(2-nitrophenyl)-3,5-pyridinedicarboxylic acid dimethyl ester Tomlinson *et al.*, 1993), is included in stimulation buffer, 50 μM glutamate application induces potentiation of Ca^{2+} influx, which does not differ significantly from the control one, without nifedipine (**Figure 29, Table 12**). In electrophysiological studies, electrical stimulation induced VGCC-dependent LTP. Thus, Izumi and Zorumski (1998), Norris *et al.* (1998), Grover (1998) and Shankar *et al.* (1998) have proved that tetanus- or theta-burst-induced LTP in CA1 neurons of rat hippocampal slices have two components: NMDAR-dependent one (blocked by NMDAR antagonists AP-5 and MK-801) and L-type VGCC-dependent one (blocked by nifedipine). These studies provided also evidence that relative contribution of the two LTPs correlates with age. Data from Shankar *et al.* (*ibid.*) demonstrated that VGCC-dependent LTP becomes dominant in slices form old (24 months) rats, whereas in younger animals the NMDAR-dependent component is the dominant one. (For comparison, it should be noted that, on the day of preparation, rats in our experiments were 2-3 days old.) Studies of Wang *et al.* (1997) on dentate gyrus neurons and Cavuº and Teyler (1996) on cells from CA1 region suggested that in these two hippocampal regions NMDAR LTP and VGCC LTP might share (dentate gyrus) and not share (CA1) common intracellular signal transduction pathways.

4.4 Modulation of glutamate-induced potentiation by nicotine and galanthamine

Nicotine has been shown to have profound influence on tetanus-induced, hippocampal LTP (Wayner *et al.*, 1996; Fujii *et al.*, 2000a; Fujii *et al.*2000b, Fujii *et al.*, 1999). Link between GluR-dependent plasticity phenomena and nicotine might be very important, since the latter is able to enhance cognitive functions by an unknown mechanism (*ibid.*). However, we

could not observe any nicotine-induced increase in calcium concentration, although the hippocampal cells were shown to have α-7 nAChRs (Mike *et al*., 2000). This contradiction might be due to the fact that α-7 nAChRs nAChR agonists (including nicotine) are potent agents of receptor desensitization (Briggs and McKenna, 1998). Thus, agonist concentrations that elicited only 0.6-1.2% nAChR activation were sufficient to inhibit the response to ACh by 50% (*ibid.*). Additionally, our signal acquisition system lagged about a second behind the stimulus application. Provided that hippocampal nAChRs desensitise very quickly, calcium that could have entered the cell would be probably buffered out prior to cell illumination.

Nicotine effects that we were able to measure (i.e. modulation of 50 μM glutamate-induced potentiation by 100 μM nicotine: **Figure 29, Table 13**) could be partly explained by conclusions from the studies mentioned above. Recent publications of Fujii and the colleagues demonstrate the ability of nicotine to positively modulate LTP by additional stimulation of pyramidal neurons in at least two ways: 1) by activation of non-α7 nAChRs, and 2) by inactivation (desensitisation) of α7 nAChR.

Both of these activities further inactivate GABAergic interneurons, which adds up even more to a pro-LTP effect. This is in good accordance with our data, as far as the nicotine-positive cell population is concerned. In the cases where nicotine co-application correlates to reversal of potentiation, more additional research is required. The same is true for the possible direct influence of galanthamine on potentiation. The mean value of calcium influx enhancement if 0.5 μM galanthamine is coapplied with 50 μM glutamate is 2.19 times bigger than control potentiation (glutamate only) indeed (**Figures 31, Table 15**), but the dispersion of potentiation intensity among the galanthamine-treated cells is so huge (**Figure 32**) that cell-to-cell approach might seem more promising. So far, very little is known about possible action of anti-cholinesterase compounds on glutamateregic systems. A binding study, published by Wang *et al.* in 1999, has suggested that cholinesterase inhibitors might exhibit an antagonist effect on NMDARs, ranging in IC_{50} values from 36.9 μM for tacrine to 3.3 mM for galanthamine. This means that, at concentrations approximately four orders of magnitude larger than the ones we used (0.5 μM), galanthamine would **inhibit** induction of LTP.

4.5 Conclusion

Our work has shown that fluorescence microscopy of a primary hippocampal cell culture system can be used as a research tools for synaptic plasticity phenomena (LTP), with the po-

tential to provide complementary information to the one obtained by means of electrophysiology, enabling measurements of intracellular - temporal and spatial - ion dynamics. Since ion dynamics is an important indicator of the physiological state of the cell, it could be used as a source of preliminary information for *e.g.* functional proteomics. Additionally equipped by immunofluorescence data, cell subtype statistical analysis could be easily performed as well, thus compensating for lack of cellular organisation in comparison with tissue slices. System adjustment to imaging of organised structures – *e.g.* tissue slices – would be also possible (Yuste, 2000). The application example of nicotine- and galanthamine-modulated potentiation suggests how this approach might provide additional insight into various aspects of neuronal cell physiology and patophysiology.

5. SUMMARY AND PERSPECTIVE

This work's aim was to test whether LTP-like features can also be measured in cell culture and by methods that allow to analyse a alrger number of cells. A suitable method for this purpose is calcium imaging. The rationale for this approach lies in the fact that LTP/LTD are dependent on changes in intracellular calcium concentrations. Calcium levels have been measured using the calcium sensitive dye fura-2, whose fluorescence spectrum changes upon formation of the [fura-2-Ca^{2+}] complex.

Our LTP-inducing protocol comprised of two glutamate stimuli of identical size and duration (50 µM, 30 s) which were separated by 35 min. We could demonstrate that such a stimulation pattern gives rise to approx. 25% larger calcium influx at the second stimulus. It has been shown than such a stimulation pattern gives rise to an average of 25% augmentation (potentiation) of the second response, with 69% of potentiated cells. This experimental paradigm shows the pharmacological properties of LTP, established by previous electrophysiological studies:

- blocking of NMDARs and mGluRs eliminates LTP induction;
- blocking of AMPARs and L-type VGCCs does not eliminate LTP induction.

Having obtained a system for induction and following of LTP-like changes, a preliminary application example was performed. Its purpose was to investigate possible influence of nicotine and galanthamine on our potentiation effect. Nicotine (100 µM) was shown both to increase and to eliminate glutamate-induced potentiation. Galanthamine coapplication (0.5 µM) with nicotine and glutamate exerted no effect on nicotinic modulation. However, galanthamine coapplied with glutamate alone seems to augment glutamate-induced potentiation.

An LTP model system presented here could be additionally refined, by variation of glutamate application times, and testing for dependence on various forms of protein kinases. Galanthamine effect would probably be better addressed by cell-to-cell measurements instead of statistical approach, with subsequent identification of the cell type. Alternatively, combined calcium imaging – electrophysiological experiments could be performed.

Spatial and temporal properties of intracellular ion dynamics could be utilised as diagnostic tools of the physiological state of the cells, thereby finding its application in functional proteomics.

6. BIBLIOGRAPHY

Abe K., Saito H: Epidermal Growth Factor Selectively Enhances NMDA Receptor-Mediated Increase of Intracellular Ca^{2+} concentration in Rat Hippocampal Neurons *Brain Res.* 1992 (**587**) 1 102-108

Abraham W.C., Mason S.E: Effects of the NMDAR Channel Antagonist CPP and MK-801 on Hippocampal Field Potentials and Long-Term Potentiation in Anaesthetised Rats *Brain Res.* 1988 (**462**) 40-46

Alberca R., Gil-Néciga E., Salas D., Pérez J.A., Lozano P.: Psychoptic Symptoms and Alzheimer's Disease *Neurologia* 2000 (**15**) 8-14

Alger B.E., Teyler T.J: Long-Term and Short-Term Plasticity in the CA1, CA3 and Dentate Regions of the Rat Hippocampal Slice *Brain Res.* 1976 (**110**) 463-480

Aniksztejn L., Otani S., Ben-Ari Y: Quisqualate Metabotropic Receptors Modulate NMDA Currents and Facilitate Induction of Long-Term Potentiation Through Protein Kinase C *Eur. J. Neurosci.* 1992 (**4**) 500-505

Arendash G.W., Sanberg P.R:, Senqstock G.J.: Nicotine Enhances the Learning and Memory of Aged Rats *Pharmacol. Biochem. Behav.* 1995 (**29**) 517-523

Artola A., Singer W: Long-Term Depression of Excitatory Synaptic Transmission and its Relationship to Long-Term Potentiation *Trends Neurosci.* 1993 (**16**) 480-487

Ascher P., Johnson J.W.: The NMDA Receptor, its Channel and its Modulation by Glycine in: The NMDA Receptor, 2nd Ed. Editors: Collingridge G.L. and Watkins, J.C. Oxford University Press 1994 Chapter 7

Barger S.W: Complex Influence of the L-Type Calcium Channel Agonist BayK8644(+/-) on N-Methyl-D-Aspartate Responses and Neuronal Survival *Neuroscience* 1999 (**89**) 1 101-108

Bashir Z.I., Alford S., Davies S.N., Randall A.D., Collingridge G.L: Long-Term Potentiation of NMDA Receptor-Mediated Synaptic Transmission in the Hippocampus *Nature* 1990 (**349**) 156-158

Bashir Z.I., Bortolotto Z.A., Davies, C.H. *et al*: Induction of LTP in the Hippocampus Needs Synaptic Activation of Glutamate Metabotropic Receptors *Nature* 1993 (**363**) 347-350

Bazan N.G.: The Neuromessenger Platelet-Activating Factor in Plasticity and Neurodegeneration *Prog. Brain. Res.* 1998 (**118**) 281-291

Bear M.F., Connors B.W., Paradiso M: Neuroscience – Exploring the Brain Lippincott Williams and Wilkins 1995, p. 594

Behnisch T., Reymann K.G: Co-activation of Metabotropic Glutamate and N-Methyl-D-Aspartate Receptors is involved in Mechanisms of Long-Term Potentiation *Neuroscience* 1992 (**51**) 37-47

Belhage B., Frandsen A., Schousboe A.: Temporal and spatial differences in intracellular Ca^{2+} changes elicited by K^{+} and glutamate in single cultured neocortical neurons *Neurochem. Int*. 1996 (**29**) 247-253

Birks J.S., Melzer D.: Donepezil for Mild and Moderate Alzheimer's Disease *Cochrane Database Syst Rev* 2000 **:2** CD001190

Bliss, T.V., Collingridge, G.L.: A Synaptic Model for Memory: Long-Term Potentiation in the Hippocampus *Nature* 1993 (**361**) 31-39

Bortolotto Z.A., Bashir Z.I., Davies C.H., Collingridge G.L: A Molecular Switch Activated by Metabotropic Glutamate Receptors Regulates Induction of Long-Term Potentiation 1994 *Nature* (**362**) 740-743

Bortolotto Z.A., Collingridge G.L: Evidence That a Novel Metabotropic Glutamate Receptor Mediates the Induction of Long-Term Potentiation at CA1 Synapses in the Hippocampus *Biochem. Soc. Trans.* 1999 (**27**) 170-174

Brewer G.J. : Serum-Free B-27/Neurobasal Medium Supports Differentiated Growth of Neurons from the Striatum, Substantia Nigra, Septum, Cerebral Cortex, Cerebellum and Dentate Gyrus *J. Neurosci. Res*. 1995 (**42**) 674-683

Briggs C.A:, McKenna D.G.: Activation and Inhibition of the Human alpha7 Nicotinic Acetylcholine Receptor by Agonists *Neuropharmacology* 1998 (**37**) 1095-1102

Burgard E.C., Hablitz J.J.: N-Methyl D-Aspartate Receptor-Mediated Calcium Accumulation in Neocortical Neurons 1995 *Neuroscience* (**69**) 351-362

Cavuº I., Teyler T.: Two Forms of Long-Term Potentiation in Area CA1 Activate Different Signal Transduction Cascades *J. Neurophysiol*. 1996 (**76**) 3038-3047

Chen L.J., Chen R.Z.: Subtypes of Central Nicotinic Receptors Involved in Learning and Memory *Chung Kuo Yao Li Hsueh Pao* 1999 (**20)** 725-728

Churn S.B., Limbrick D., Sombati S., DeLorenzo R.J.: Excitotoxic Activation of the NMDA Receptor Results in Inhibition of Calcium/Calmodulin Kinase II Activity in Cultured Hippocampal Neurons *J. Neurosci.* 1995 (**15**) 3200-3214

Coan E.J., Collingridge G.L: Effects f Phenylcyclidine, SKF 10,047 and Related Psychotomimetic Agents on N-Methyl-D-Aspartate Mediated Synaptic Responses in Rat Hippocampal Slices *Br. J. Pharmacol*. 1987 (**91**) 547-556

Colino A., Malenka, R.J: Mechanisms Underlying Induction of Long-Term Potentiation in Rat Medial and Lateral Perforant Paths *In Vitro* *J. Neurophysiol.* 1993 (**69**) 1150-1159

Collingridge G.L., Kehl S.J., McLennan H: The Antagonism of Amino-Acid-Induced Excitations of Rat Hippocampal CA1 Neurons *In Vitro* *J. Physiol.* 1983a (**334**) 19-31

Collingridge G.L., Kehl S.J., McLennan H: Excitatory Amino Acids in Synaptic Transmission in the Schaffer Collateral-Commissural Pathway of the Rat Hippocampus *J. Physiol.* 1983b (**334**) 33-46

Collingridge G.L., Herron C.E:, Lester R.A.: Synaptic Activation of N-Methyl-D-Aspartate Receptors in the Schaffer Collateral-Commissural Pathway of Rat Hippocampus *J. Physiol. (Lond)* 1988 (**399**) 283-300

Collingridge G.L., Herron C.E:, Lester R.A.: Frequeny-Dependent N-Methyl-D-Aspartate Receptor-Mediated Synaptic Transmission in Rat Hippocampus *J. Physiol. (Lond)* 1988 (**399**) 301-312

Copelman C.A:, Cuzner M.L., Groome N., Diemel L.T.: Temporal Analysis of Growth Factor mRNA Expression in Myelinating Rat Brain Aggregate Cultures: Increments in CNTF, FGF-2, IGF-I, and PDGF-AA mRNA are Induced by Antibody-Mediated Demyelination *Glia* 2000 (**30**) 342-351

Cormier R.J., Mauk M.D., Kelly P.T: Glutamate Iontophoresis Induces Long-Term Potentiation in the Absence of Evoked Presynaptic Activity *Neuron* 1993 (**10**) 907-919

Davies S.N., Lester R.A., Reymann K.G., Collingridge G.L: Temporally Distinct Pre- and Post-synaptic Mechanisms Maintain Long-Term Potentiation *Nature* 1988 (**338**) 500-503

Debray C., Diabira D., Gaiarsa J.L., Ben-Ari Y., Gozlan H: Contributions of AMPA and GABA(A) Receptors to the Induction of NMDAR-Dependent LTP in CA1 *Neurosci. Lett.* 1997 (**238**) 119-122

van Dujin, C.M., Hofman, A.: Relation Between Nicotine Intake and Alzheimer's Disease *BMJ* 1991 (**302**) 1491-1494

Errington M.L., Lynch M.A., Bliss T.V.P: Long-Term Potentiation in the Dentate Gyrus: Induction and Increased Glutamate Release are Blocked by D-(-) Aminophosphonovalerate *Neuroscience* 1987 (**20**) 279-284

Fitzjohn S.M., Bortolotto Z.A., Palmer M.J., Doherty A.J., Ornstein P.L., Schoepp D.D., Kingston A.E., Lodge D., Collingridge G.L: The Potent mGlu Receptor Antagonist LY341495 Indentifies Roles for Both Cloned and Novel mGlu Receptors in Hippocampal Synaptic Plasticity *Neuropharmacology* 1998 (**37**) 1270-1276

Fazeli S., Collingridge G. (Editors): Cortical Plasticity LTP and LTD Bios Scientific Publishers Ltd. 1996

Fujii S., Ji Z., Morita N., Sumikawa K.: Acute and Chronic Nicotinic Exposure Differentially Facilitate the Induction of LTP *Brain Res.* 1999 (**846**) 1 137-143

Fujii S., Ji Z., Sumikawa K.: Inactivation of alpha7 ACh Receptors and Activation of non-alpha7 ACh Receptors Both Contribute to Long Term Potentiation Induction in the Hippocampal CA1 Region *Neurosci. Lett.* 2000 **286** 134-138

Fujii S., Yia Y., Yang A., Sumikawa K.: Nicotine Reverses GABAergic Inhibition of Long-Term Potentiation Induction in the Hippocampal Region *Brain Res.* 2000 **863** 259-265

Fulton B., Benfield P.: Galanthamine *Drugs Aging* 1996 (**9**) 60-65

Gamberino W.C., Gold M.S.: Neurobiology of Tobacco Smoking and Other Additive Disorders *Psychiatr. Clin. North Am.* 1999 (**22**) 302-312

Gähwiler B.H., Thompson S.T., McKInney A.R., Debanne D., Robertson R.T.: Organotypic Slice Culture of Neural Tissue in: Culturing Nerve Cells, 2nd Ed. Editors: Banker, G. and Goslin,K. MIT Press 1998 pp. 461-498

Gray C.W., Patel A.J.: Neurodegeneration Mediated by Glutamate and Beta-Amyloid Peptide: a Comparison and Possible Interaction *Brain Res.* 1995 (**691**) 169-179

Greengard P., Jen J., Nairn J.C., Stevens C.F: Enhancement of the Glutamate Response by cAMP-Dependent Protein Kinase in Hippocampal Neurons *Science* 1991 (**253**) 1135-1138

Grewal P., Yoshida T., Finch C.E., Morgan T.E.: Scavenger Receptor mRNAs in Rat Brain Microglia are Induced by Kainic Acid Lesioning and by Cytokines *Neuroreport* 1997 (**8**) 1077-1081

Grover, L.M.: Evidence for Postsynaptic Induction and Expression of NMDA Receptor Independent LTP *J. Neurophysiol.* 1998 (**79**) 1167-1182

Grynkiewicz, G., Poenie, M., Tsien, R.Y: A New Generation of Ca^{2+} Indicators with Greatly Improved Fluorescence Properties *J. Biol. Chem.* 1985 (**260**) 3440-3450

Hansel C., Artola A., Singer W: Relation Between Dendritic Ca^{2+} Levels and the Polarity of Synaptic Long-Term Modifications in Rat Visual Cortex Neurons *Eur. J. Neurosci.* 1997 (**9**) 11 2309-2322

Hansen, C.A., Monck, J.R., Williamson, J.R: *Meth. Enzymol.* 1991

Harris E.W., Cotman C.W: Long-Term Potentiation of Guinea-Pig Mossy Fibre Responses is not Blocked by N-Methyl-D-Aspartate Antagonists *Neurosci. Lett.* 1986 (**70**) 132-137

Haugland R.P: Molecular Probes – Handbook of Fluorescent Probes and Research Chemicals 7th Ed., 1999

Hayashi H., Miyata H.: Fluorescence Imaging of Intracellular Ca^{2+} *J. Pharmacol. Toxicol. Methods* 1994 (**31**) 1-10

Hebb, D.O. Organization of Behaviour; A Neuropsychological Theory. 1949

Herron C.E., Lester R.A., Coan E.J., Collingridge G.L.: Intracellular Demonstration of an N-Methyl-D-Aspartate Receptor Mediated Component of Synaptic Transmission in the Rat Hippocampus *Neurosci. Lett*. 1985 (**60**) 19-23

Hidalgo A., Urban J., Brand A.H.: Targeted Ablation of Glia Disrupts Axon Tract Formation in the Drosophila CNS *Development 1995* (**121**) 3703-3712

Higgins, D., Banker, G.: Primary Dissociated Cell Cultures in: Culturing Nerve Cells, 2nd Ed. Editors: Banker, G. and Goslin,K. MIT Press 1998 pp. 37-78

Hof P.R., Cox K., Morrison J.H. (a): Quantitative Analysis of a Vulnerable Subset of Pyramidal Neurons in Alzheimer's Disease: I. Superior Frontal and Inferior Temporal Cortex. *J Comp Neurol* 1990 (**301**) 44-54

Hof P.R., Cox K., Morrison J.H. (b): Quantitative Analysis of a Vulnerable Subset of Pyramidal Neurons in Alzheimer's Disease: II. Primary and secondary visual cortex. *J Comp Neurol* 1990 (**301**) 55-64

Honoré T., Davies S.N., Drejer J., Fletcher E.J., Jacobsen P., Lodge D., Nielsen F.E.: Quinoxalinediones: Potent Competitive non-NMDA Glutamate Receptor Antagonists *Science* 1988 (**241**) 701-703

Hoyert D.L., Rosenberg H.M.: Alzheimer's Disease as a Caouse of Death in the United States *Public Health Rep.* 1997 (**112**) 497-505

Hoyert D.L., Rosenberg H.M.: Mortality from Alzheimer's Disease: an Update. *Natl. Vital. Stat. Rep.* 1999 (**47**) 1-8

Hu G.Y., Hvalby O., Walaas S.I., Albert K.A., Skjeflo P., Andersen P., Greengard P.: Protein Kinase C Injection into Hippocampal Pyramidal Cells Elicits Features of Long-Term Potentiation *Nature* 1987 (**328**) 426-429

Huang Y.Y., Kandel, E.R.: Recruitment of Long-Lasting and Protein Kinase A-Dependent Long-Term Potentiation in the CA1 Region of Hippocampus Requires Repeated Retanization *Learn. Mem.* 1994 (**1**) 74-82

Huang Y.Y., Malenka R.C: Examination of TEA-Induced Synaptic Enhancement in Area CA1 of the Hippocampus: the Role of Voltage-Dependent Ca^{2+} Channels in the Induction of LTP *J. Neurosci*. 1993 (**13**) 568-576

Huber K.M., Mauk M.D., Kelly P.T: Distinct LTP Induction Mechanisms: Contribution of NMDA Receptors and Voltage-Dependent Calcium Channels. *J. Neurophysiol*. 1995 (**73**) 270-279

Hunter B.E., de Fiebre C.M., Papke R.L., Kern W.R., Meyer E.M.: A Novel Nicotinic Agonist Facilitates Induction of Long-Term Potentiation in the Rat Hippocampus *Neurosci. Lett*. 1994 (**168**) 130-134

Isomura Y., Kato N: Action Potential-Induced Dendritic Calcium Dynamics Correlated with Synaptic Plasticity in Developing Hippocampal Pyramidal Cells *J. Neurophysiol*. 1999 (**82**) 4 1993-1999

Izumi Y., Miyakawa H., Ito K, Kato H: Quisqualate and N-methyl-D-aspartate (NMDA) in Induction of Hippocampal Long-Term Facilitation Using Conditioning Solution *Neurosci. Lett*. 1987 (**83**) 201-206

Izumi Y., Zorumski C.F: LTP in CA1 of the Adult Rat Hippocampus and Voltage-Activated Calcium Channels *Neuroreport* 1998 (**9**) 3689-3691

Jaffe D.B., Brown T.H: Confocal Imaging of Dendritic Ca^{2+} transients in Hippocampal Brain Slices During Simultaneous current- and voltage-clamp recording *Micros. Res. Tech.* 1994 (**29**) 4 279-289

Jane D.E., Olverman H.J., Watkins J.C.: Agonists and Competitive Antagonists: Structure-Activity and Molecular Modelling Studies in: The NMDA Receptor, 2nd Ed. Editors: Collingridge G.L. and Watkins, J.C. Oxford University Press 1994 Chapter 2

Jay T.M., Zilkha E., Obrenovitch T.P.: Long-Term Potentiation in the Dentate Gyrus is not Linked to Increased Extracellular Glutamate Concentration *J. Neurophysiol*. 1999 (**81**) 1741-1748

Kandel E.R., Schwartz J.H., Jessell T.M.: Principal of Neural Science 4th Ed. p.20 McGraw Hill 2000

Kao J.P.Y: Practical Aspects of Measuring $[Ca^{2+}]$ with Fluorescent Indicators *Meth. Cell Biol.* 1994 (**40**) 155

Kauer J.A., Malenka R.C., Nicoll R.A: A Persistent Postsynaptic Modification Mediates Long-Term Potentiation in the Hippocampus *Neuron* 1988 (**1**) 911-917

Kendrick K.M., Guevara-Guzman R., Zorrilla J., Hinton M.R., Broad K.D., Mimmack M., Ohkura S.: Formation of Olfactory Memories Mediated by Nitric Oxide *Nature* 1997 (**388**) 670-674

Kingston A.E., Ornstein P.L., Wright R.A., Johnson B.G., Mayne N.G., Burnett J.P., Belagaje R., Wu S., Schoepp D.: LY341495 is a Nanomolar Potent and Selective Antagonist of Group II Metabotropic Glutamate Receptors *Neuropharmacology* 1998 (**37**) 1-12

Klann E., Chen S.J., Sweatt J.D.: Persistent Protein Kinase Activation in the Maintenance Phase of Long-Term Potentiation *J. Biol. Chem*. 1991 (**266**) 24253-24256

Klann E., Chen S.J., Sweatt J.D.: Mechanism of Protein Kinase C Activation During the Induction and Maintenance of Long-Term Potentiation Probed Using a Selective Peptide Substrate *Proc. Natl. Acad. Sci. U.S.A.* 1993 (**90**) 8337-8341

Knöpfel T., Kuhn R., Allgeier H.: Metabotropic Glutamate Receptors: Novel Targets for Drug Development *J. Med. Chem.* 1995 (**38**) 1417-1426

Koh D.S., Geiger J.R., Jonas P., Sakmann B.: Ca^{2+}-Permeable AMDA and NMDA Receptor Channels in Basket Cells of Rat Hippocampal Dentate Gyrus *J. Physiol. (Lond.)* 1995 (**485**) 383-402

Larkum M.E., Warren D.A., Bennett M.R: Calcium Concentration Changes in the Calyciform Nerve Terminal of the Avian Cilliary Ganglion After Tetanic Stimulation *J. Auton. Nerv. Syst*. 1994 (**46**) 3 175-188

Lee H.-K., Kameyama K., Huganir R.L., Bear M.F: NMDA Induces Long-Term Synaptic Depression and Dephosphorylation of the GluR1 Subunit of AMPA Receptors in Hippocampus *Neuron* 1998 (**21**) 1151-1162

Lee J.-M., Zipfel G.J., Choi, D.W: The Changing Landscape of Ischaemic Brain Injury Mechanisms *Nature (Suppl.)* 1999 (**399**) 6738

Lisman, J: A Mechanism for the Hebb and the Anti-Hebb Processes Underlying Learning and Memory *Proc. Natl. Acad. Sci. USA* 1989 (**86**) 9574-9578

Liu J., Fukunaga K., Yamamoto H., Nishi K., Miyamoto E.: Differential Roles of Ca^{2+}/Calmoduline-Dependent Protein Kinase II and Mitogen-Activated Protein Kinase Activation in Hippocampal Long-Term Potentiation *J. Neurosci.* 1999 (**19**) 8292-8299

Lovinger D.M., Wong K.L., Murakami K., Routtenberg A.: Protein Kinase C Inhibitors Eliminate Hippocampal Long-Term Potentiation 1987 *Brain Res.* (**436**) 177-183

Lynch M.A., Errington M.L., Bliss T.V.: The Increase in [^{3}H]Glutamate Release Associated with Long-Term Potentiation in the Dentate Gyrus is Blocked by Commissural Stimulation *Neurosci. Lett.* 1989 (**103**) 191-196

Malgaroli A., Tsien R.W: Glutamate-Induced Long-Term Potentiation of the Frequency of Miniature Synaptic Currents in Cultured Hippocampal Neurons *Nature* 1992 (**357**) 134-139

Malinow R: LTP: Desperately Seeking Resolution *Science* 1994 (266) 1195-1196

Malinow R., Madison D.V., Tsien R.W.: Persistent Protein Kinase Activity Underlying Long-Term Potentiation 1988 *Nature* (**335**) 820-824

Maren S., Baudry M., Thompsen R.F: Differential Effects of Ketamine and MK-801 on the Induction of Long-Term Potentiation *NeuroReport* 1991 (**2**) 239-242

Martini R., Schachner M.: Molecular Bases of Myelin Formation as Revealed by Investigations on Mice Deficient in Glial Cell Surface Molecules *Glia* 1997 (**19**) 298-310

McGlade-McCullogh E., Yamamoto H., Tan S.-E., Brickley D.A., Soderling T.L: Phosphorylation and Regulation of Glutamate Receptors by Calcium/Calmodulin-Dependent Protein Kinase II *Nature* 1993 (**362**) 640-642

McGuinness N., Anwyl R., Rowan M.J: *Trans*-ACPD Enhances Long-Term Potentiation in the Hippocampus *Eur. J. Pharmacol.* 1991 (**197**) 231-232

Mike A., Pereira E.F., Albuquerque E.X.: Ca^{2+}-Sensitive Inhibition by Pb^{2+} of alpha7-Containing Nicotinic Acetylcholine Receptors in Hippocampal Neurons *Brain Res.* 2000 (**873**) 112-123

Miller R.J., Bindokas V.P., Babcock D.F., Lee J.-P., Jordan, J.B: Factors Regulating Excitotoxic Neurodegeneration: The Role of Calcium and the Mitochondria 1998 *Excitatory Amino Acids: From Genes to Therapy* Eds: Seeburg P.H., Bresink I., Turski L. Springer Verlag pp. 43-64

Minota S., Kumamoto E., Kitakoga O., Kuba K: Long-Term Potentiation Induced by a Sustained Rise in the Intraterminal Ca^{2+} in Bull-Frog Sympatetic Ganglia *J. Physiol. (London)* 1991 (**435**) 421-438

Morris R.G.M., Anderson E., Lynch G.S., Baudry M: Selective Impairment of Learning and Blockade of LTP by NMDA receptor antagonist, AP5. *Nature* 1986 (**319**) 774-776

Musleh W., Bi X., Tocco G., Yaghoubi S., Baudry M: Glycine-Induced Long-Term Potentiation is Associated With Structural and Functional Modifications of α-amino-3-hydroxyl-5-methyl-4-isoxazolepropionic acid receptors *Proc. Natl. Acad. Sci. USA* 1997 (**94**) 9451-9456

Motulsky, H.: Intuitive Biostatistics Oxford University Press 1995

Neveu D., Zucker R.S (a): Postsynaptic Levels of $[Ca^{2+}]_i$ Needed to Trigger LTP and LTD *Neuron* 1996 (**16**) 619-629

Neveu D., Zucker R.S (b): Long-lasting Potentiation and Depression Without Presynaptic Activity *J. Neurophysiol.* 1996 (**75**) 2157-2160

Nicholls J.G., Martin A.R., Wallace B.G.: From Neuron to Brain: A Cellular and Molecular Approach to the Function to the Function of the Nervous System, 3rd Ed. Sunderland MA:Sinauer 1992

Nordberg A.: Neuroreceptor Changes in Alzheimer Disease *Cerebrovasc. Brain Metab. Rev.* 1992 (**4**) 303-328

Norris C.M., Halpain S., Foster T.C.: Reversal of Age-Related Alterations in Synaptic Plasticity by Blockade of L-Type Ca^{2+} Channels *J. Neurosci.* 1998 (**18**) 3171-3179

Oliver, M.W., Schacklock J.A., Kessler M., Lynch G., Baimbridge K.G: The Glycine Site Modulates NMDA-Mediated Changes of Intracellular Free Calcium in Cultures of Hippocampal Neurons *Neurosci. Lett*. 1990 (**114**) 2 197-202

Ouyang Y., Rosenstein A., Kreiman G., Schuman E.G., Kennedy M.B.: Tetanic Stimulation Leads to Increased Accumulation of Ca^{2+}/Calmodulin-Dependent Protein Kinase II *via* Dendritic Protein Synthesis in Hippocampal Neurons *J. Neurosci.* 1999 (**19**) 7823-7833

Patneau D.K., Mayer M.L.: Structure-Activity Relationships for Amino Acid Transmitter Candidates Acting at N-Methyl-D-Aspartate and Quisqualate Receptors *J. Neurosci*. 1990 (**10**) 2385-2399

Park D.S., Morris E.J., Stefanis L., Troy C.M., Shelanski M.L., Geller H.M., Greene L.A.: Multiple Pathways of Neuronal Death Induced by DNA-Damaging Agents, NGF Deprivation, and Oxidative Stress *J. Neurosci*. 1998 (**18**) 830-840

Parton R.M., Read N.D.: Calcium and pH Imaging in Living Cells in: Light Microscopy in Biology: A Practical Approach 2nd Edition Editor: Lacey A.J. Oxford Univeristy Press 1999 p. 221 -271

Petr M.J., Wurster R.D: Determination of *in Situ* Dissociation Constant for Fura-2 and Quantitation of Background Fluorescence in Astrocyte Cell Line U373-MG *Cell Calcium* 1997 (**21**) 233

Petrozzino J.J., Connor J.A: Dendritic Ca^{2+} accumulation and metabotropic glutamate receptor activation associated with an N-Methyl-D-Aspartate Receptor-Independent Long-Term Potentiation in Hippocampal CA1 Neurons *Hippocampus* 1994 (**4**) 5 546-558

Poenie M., Tsien, R.: Fura-2: A Powerful New Tool for Measuring and Imaging $(Ca^{2+})_i$ in Single Cells Prog. Clin. Biol. Res. 1986 (**53**) 210-

Porter J.T., McCarthy K.D.: Hippocampal Astrocytes *in situ* Respond to Glutamate Released from Synaptic Terminals 1996 *J. Neurosci.* (**16**) 5073-5081

Powell C.M., Johnston D., Sweatt J.D.: Autonomously Acitve Protein Kinase C in the Maintenance Phase of N-Methyl-D-Aspartate Receptor-Independent Long-Term Potentiation *J. Biol. Chem*. 1994 (**269**) 27958-27963

Qizilbash N., Birks J., López-Arrieta J., Lewington S., Szeto S.: Tacrine for Alzheimer's Disease *Cochrane Database Syst Rev* 2000 **:2** CD000202

Radcliffe K.A., Dani J.A.: Nicotinic Stimulation Produces Multiple Forms of Increased Glutamate Synaptic Transmission *J. Neurosci*. 1998 (**18**) 7075-7083

Regher W.G., Atluri P.P: Calcium Transients in Cerebellar Granule Cell Presynaptic Terminals *Biophys.J*. 1995 (**68**) 2156

Regher W.G., Tank D.W: The Maintenance of LTP at Hippocampal Mossy Fiber Synapses is Independent of Sustained Presynaptic Calcium *Neuron* 1991 (**7**) 3 451-459

Revest, P, Longstaff, A.: Molecular Neuroscience Bios Scientific Publishers 1998

Reyes, M., Stanton, P.K.: Induction of Hippocampal Long-Term Depression Requires Release of Ca^{2+} from Separate Presynaptic and Postsynaptic Intracellular Stores *J. Neurosci.* 1996 (**16**) 5951-5960

Reymann K.G., Matthies H: 2-Amino-4-Phosphonobutyrate Selectively Eliminates Late Phase of Long-Term Potentiation in Rat Hippocampus *Neurosci. Lett.* 1989 (**98**) 166-171

Riederer P., Jellinger K.: Morphological and Biochemical Changes in the Ageing Brain: Patophysiological and Possible Therapeutic Consequences *Exp. Brain. Res*. 1982 **Suppl. 5** 158-166

Roe, M.W., Lemasters J.J., Herman, B: Assessment of Fura-2 for Measurements of Cytosolic Free Calcium *Cell Calcium* 1990 **11** 63-73

Fluorescent Probes *Cell Biology: A Laboratory Handbook*, 2nd Ed., Vol. 3, Ed. Celis, J.E., 1998 (**364**) pp. 363

Sawada S., Yamamoto C., Ohno-Shosaku T.: Long-Term Potentiation in the Dentate Gyrus, and the Effects of Nicotine *Neurosci. Res.* 1994 (**20**) 323-329

Schrattenhloz A., Pereira E.F.A., Roth U., Weber K.-H., Albuquerque E., Maelicke, A. : Agonist Responses of Neuronal Nicotinic Acetylcholine Receptors Are Potentiated by a No vel Class of Allosterically Acting Ligands M*ol. Pharmacol*. 1996 **49** 1-6

Schwartswelder H.S., Ferrari C., Anderson W.W., Wilson W.A: The Drug MK-801 Attenuates the Development, But not the Expression, of Long-Term Potentiation and Stimulus Train-Induced Bursting in Hippocampal Slices *Neuropharmacology* 1988 (**28**) 441-445

Sessoms J.S., Chen S.J., Chetkovitch D.M., Powell C.M., Roberson E.D., Sweatt J.D., Klann E.: Ca^{2+}-Induced Persistent Protein Kinase C Activation in Rat Hippocampal Homogenates 1992-93 *Second Messengers Phosphoproteins* (**14**) 109-126

Shankar S., Teyler T.J., Robbins N: Aging Differentially Alters Forms of Long-Term Potentiation in Rat Hippocampal Area CA1 *J. Neurophysiol.* 1998 (**79**) 334-341

Shelton M.K., McCarthy K.D.: Mature Hippocampal Astrocytes Exhibit Functional Metabotropic and Ionotropic Glutamate Receptors *in situ* *Glia* 1999 (**26**) 1-11

Shepherd, M: The Synaptic Organisation of the Brain, 4th Ed. 1998 Oxford University Press

Sliver R.B.: Ratio Imaging: Practical Considerations for Measuring Intracellular Calcium and pH in Living Tissue *Meth.Cell Biol*. 1998 (**56**) 237

Son H., Carpenter D.O.: Interactions Among Paired-Pulse Facilitation and Post-Tetanic and Long-Term Potentiation in the Mossy Fiber – CA3 Pathway in Rat Hippocampus *Synapse* 1996 (**23**) 302-311

Stevens C.F., Tonegawa S., Wang Y.: The Role of Calcium-Calmodulin Kinase II in Three Forms of Synaptic Plasticity *Curr. Biol.* 1994 (**4**) 687-693

Stringer J.L., Guyenet P.G: Elimination of Long-Term Potentiation in the Hippocampus by Phenylcyclidine and Ketamine *Brain Res.* 1983 (**258**) 159-164

Stringer J.L., Greenfield L.J., Hackett J.T., Guyenet P.G: Blockade of Long-Term Potentiation by Phenylcyclidine and σ-Opiates in the Hippocampus *in vitro* and *in vivo* *Brain Res.* 1983a (**280**) 127-138

Stringer J.L., Hackett J.T., Guyenet P.G: Long-Term Potentiation Blocked by Phenylcyclidine and Cycloazocine *in vitro* *Eur. J. Pharmacol*. 1983b (**98**) 381-388

Swope S.L., Moss S.I., Raymond L.A., Huganir R.L.: Regulation od Ligand-Gated Ion Channels by Protein Phosphorilation *Adv. Second Messenger Phosphoprotein Res*. 1999 (**33**) 49-78

Szmacinski H., Lakowitz J.R: Possibility of Simultaneously Measuring Low and High Calcium Concentrations using Fura-2 and lifetime-based sensing *Cell Calcium* 1995 (**18**) 1 64-75

Takahashi A., Camacho P., Lechleiter J.D., Herman B.: Measurement of Intracellular Calcium *Physiol. Rev*. 1999 (**79**) 1089-1125

Tatsumi S., Katayama Y: Calcium Homeostasis in the Presence of Fura-2 in Neurons Dissociated From Rat Nucleus Basalis: Theoretical and Experimental Analysis of Chelating Action of Fura-2 *J. Neurosci. Methods* 1994 (**53**) 2 209-215

Tekkök S., Medina I., Krnjevic K: Intraneuronal [Ca^{2+}] Changes Induced by 2-Deoxy-D-Glucose in Rat Hippocampal Slices *J. Neurophysiol*. 1999 (**81**) 1 174-183

Thiels E., Weisz D.J., Berger T.W: *In Vivo* Modulation of N-Methyl-D-Aspartate Receptor-Dependent Long-Term Potentiation by the Glycine Modulatory Site *Neuroscience* 1992 (**46**) 501-509

Tomlinson W.J., Stea A., Bourinet E., Charnet P., Narqeot J., Snutch T.P.: Functional Properties of a Neuronal Class C L-type Calcium Channel *Neuropharmacology* 1993 (**32**) 1117-1126

Tsien, R: Fluorescent Probes of Cell Signaling *Ann. Rev. Neurosci*. 1989 **12** 227-253

Tsien R., Pozzan, T: Measurement of Cytosolic Free Ca^{2+} with Quin2 *Meth. Enzymol*. 1989 (**172**) 230

Tsien R., Pozzan T., Rink T.J.: Calcium Homeostasis in Intact Lymphocytes: Cytoplasmic Free Calcium Monitored with a New, Intracellularly Trapped Fluorescent Indicator *J. Cell Biol.* 1982 (**94**) 325-334

Vannucci S.J., Maher F., Simpson I.A.: Glucose Transporter Proteins in Brain: Delivery of Glucose to Neurons and Glia *Glia* 1997 (**21**) 2-21

Voronin L.L.: Quantal Analysis of Hippocampal Long_Term Potentiation *Rev. Neurosci.* 1994 (**5**) 141-170

Wang J.H., Feng T.P.: Postsynaptic Protein Kinase C Essential to Induction and Maintenance of Long-Term Potentiation in the Hippocampal CA1 Region 1992 *Proc. Natl. Acad. Sci. U.S.A.* (**89**) 2576-2580

Wang L.-Y., Salter M.W., McDonald J.F: Regulation of Kainate Receptors by cAMP-Dependent Protein Kinase and Phosphatases *Science* 1991 (**253**) 1132-1135

Wang X.-D., Chen X.-C., Yang H.-H., Hu G.-Y.: Comparison of the Effects of Cholinesterase Inhibitos on (3H)MK-801 Binding in Rat Cerebral Cortex *Neurosci. Lett*. 1999 **272** 21-24

Wang Y., Rowan M.J., Anwyl R.: LTP Induction Dependent on Activation of Ni^{2+}-Sensitive Voltage-Gated Calcium Channels, but not NMDA Receptors, in the Rat Dentate Gyrus *in vitro J. Neurophysiol.* 1998 (**78**) 2574-2581

Watkins J., Collingridge G.: Phenylglycine Derivatives as Antagonists of Metabotropic Glutamate Receptors *Trends Pharmacol. Sci*. 1994 (**15**) 332-342

Wayner M.J., Armstrong D.L., Phelix, C.F.: Nicotine Blocks Angiotensin II Inhibition of LTP in the Dentate Gyrus *Peptides* 1996 (**17**) 1127-1133

Wenzel J., Lammert G., Meyer U., Krug, M.: The Influence of Long-Term Potentiation on the Spatial Relationship Between Astrocyte Processes and Potentiated Synapses in the Dentate Gyrus Neuropil of Rat Brain *Brain Res.* 1991 (**560**) 122-131

West M.J., Coleman P.D., Flood D.G., Troncoso J.C.: Differences in the Pattern of Hippocampal Neuronal Loss in normal Ageing and Alzheimer's Disease *Lancet* 1994 (**344**) 769-772

Williams S., Johnston D: Long-Term Potentiation of Hippocampal Mossy Fiber Synapses is Blocked by Postsynaptic Injection of Calcium Chelators *Neuron* 1989 (**3**) 5 583-588

Wu L.G., Saggau P: Presynaptic Calcium is Increased During Normal Synaptic Transmission and Paired-Pulse Facilitation, but not in Long-Term Potentiation in Area CA1 of Hippocampus *J. Neurosci*. 1994 (**14**) 2 645-654

Yang S.-N., Tang Y.-G., Zucker R.S: Selective Induction of LTP and LTD by Postsynaptic $[Ca^{2+}]_i$ Elevation *J. Neurophysiol*. 1999 (**81**) 781-787

Yasuda H., Tsumoto T: Long-Term Depression in Rat Visual Cortex is Associated With a Lower Rise of Postsynaptic Calcium than Long-Term Potentiation *Neurosci. Res*. 1996 (**24**) 3 265-274

Yin H.Z., Sensi S.L., Carriedo S.G., Weiss J.G: Dendritic Localization of Ca^{2+}-permeable AMPA/kainate Channels in Hippocampal Pyramidal Neurons *J. Comp. Neurol*. 1999 (**409**) 2 250-260

Yuste R: Loading Brain Slices with AM Esters of Calcium Indicators in: **Imaging Neurons: A Laboratory Manual** Editors: Yuste R., Lanni F., Konnerth A. Cold Spring Harbor Laboratory Press 2000 Chapter 34.1

Yuste R., Denk W: Dendritic Spines as Basic Functional Units of Neuronal Integration *Nature* 1995 (**375**) 682-684

Zalutsky R.A., Nicoll R.A: Mossy Fiber Long-Term Potentiation Shows Specificity But No Apparent Cooperativity *Science* 1990 (**248**) 1619-1624

Zhang D.X., Levy W.B: Ketamine Blocks the Induction of LTP at the Lateral Etorhinal Cortex-Dentate Gyrus Synapses *Brain Res.* 1992 (**593**) 124-127

Zheng F., Gallagher J.P., Connor J.A: Activation of a Metabotropic Excitatory Amino Acid Receptor Potentiates Spike-Driven Calcium Increases in Neurons of the Dorsolateral Septum *J. Neurosci.* 1996 (**16**) 19 6079-6088

Zilberter Y.I., Uteshev V.V., Sokolova S.N., Motin L.G., Eremjan H.H: Potentiation of Glutamate-Activated Currents in Isolated Hippocampal Neurons *Neuron* 1990 (**5**) 597-602

Zucker R.S: Calcium- and Activity-Dependent Synaptic Plasticity *Curr. Op. Neurobiol.* 1999 (**9**) 305-313